SCIENTIFIC OASIS

Spectrum of Operational Research

Journal homepage: www.sor-journal.org
ISSN: 3042-1470

Power and Energy Transformation: Multi-Criteria Decision-Making Utilizing Complex q-Rung Picture Fuzzy Generalized Power Prioritized Yager Operators

Subramanian Petchimuthu[1], Fathima Banu M.[1,*], C. Mahendiran[2], T. Premala[3]

[1] Department of Science and Humanities (Mathematics), University College of Engineering Nagercoil, Anna University, Tamilnadu, India
[2] Department of Science and Humanities (Chemistry), University College of Engineering Nagercoil, Anna University, Tamilnadu, India
[3] Good Shepherd College of Engineering and Technology, Anna University, Tamilnadu, India

ARTICLE INFO

Article history:
Received 28 December 2024
Received in revised form22 January 2025
Accepted 25 January 2025
Available online 27 January 2025

Keywords:

Power and Energy; Complex q-rung Picture Fuzzy Sets; Yager's Operations; MCDM ; Fuzzy logic

ABSTRACT

Existing studies in decision-making often face limitations in adequately handling complex and uncertain environments. This study addresses these shortcomings by introducing novel operations and aggregation techniques tailored for complex q-rung picture fuzzy numbers (Cq-RPFNs). Building upon the drawbacks of conventional approaches, we extend Yeager's operations to Cq-RPFNs, enabling comprehensive operations such as addition, multiplication, scalar product, and scalar power. Additionally, two aggregation operators, the Complex q-rung Picture Fuzzy Generalized Power Prioritized Yager Weighted Average, and the Complex q-rung Picture Fuzzy Generalized Power Prioritized Yager Weighted Geometric are developed to overcome the limitations of existing aggregation methods. Rigorous analysis of these operators for properties such as idempotency and monotonicity ensures their robustness in decision-making processes. Through a comprehensive multi-criteria decision-making method utilizing these operators, decision-makers are empowered to navigate complex decision landscapes effectively. Comparative evaluations against existing alternatives highlight the superiority and effectiveness of the proposed approaches. A case study focusing on India's Power and Energy Sector in 2024 demonstrates practical application, supported by numerical examples that validate the methodologies' efficacy. This study addresses the drawbacks of existing approaches and provides valuable insights and tools for decision-makers operating in complex and uncertain domains.

*Corresponding author.
E-mail address: fathimams1999@gmail.com

https://doi.org/10.31181/sor21202525

1. Introduction

Power and energy are vital to modern society, driving everything from electricity generation to transportation. Efficient management of these resources is essential for economic growth and environmental sustainability. Readers are encouraged to refer to the Appendix (Table 15) for the abbreviation key used throughout this article. Recent advancements in energy technologies aim to address global challenges and improve energy efficiency. Bharatee et al. [1] (2022) explore hybrid energy storage systems in AC/DC microgrids for enhanced grid stability. Ghasemi et al. [2] (2023) propose an intelligent strategy to improve Micro-Grid voltage and frequency control. Bao et al. [3] (2023) focus on optimal planning for hybrid microgrid design, utilizing renewable energy effectively. Karunathilake et al. [4] (2023) discuss smart farming through advanced energy management in precision agriculture. Liu et al. [5] (2023) introduce a collaborative optimization approach for integrated energy systems. Kandpal [6] (2024) emphasizes evaluating energy solutions for global sustainability and climate change. Yu et al. [7] (2023) highlight advanced optimization techniques for addressing renewable energy intermittency. Chen et al. [8] (2023) advocate for multi-dimensional evaluations of hybrid energy systems. These studies collectively emphasize the integration of technical expertise with socio-economic considerations for sustainable energy solutions. In short, power and energy are essential to modern life.

1.1 *Motivation of the Proposed Study*

Power and energy are the cornerstones of modern civilization, driving innovation and sustainability. Transitioning from classical to smart and innovative technologies in the power and energy sectors is essential to optimize efficiency, reduce environmental impacts, and improve quality of life. Investments in smart solutions such as LED street lighting, wave energy extraction, grid technologies, and sustainable energy systems are pivotal for a resilient future.

Classical LED street lighting suffers from energy inefficiency, high maintenance costs, and limited functionality. Smart LED lighting (Figure 1) addresses these challenges by offering intelligent lighting and features like 5G/Wi-Fi hotspots, enhancing urban infrastructure and sustainability [9, 10].

Fig. 1. Comparison between Classical and Smart LED Street Lighting in Urban Environments [9, 10]

Similarly, classical wave energy systems face inefficiencies, environmental concerns, and high initial costs. Smart wave energy extraction (Figure 2) mitigates these issues, offering improved efficiency, environmental benefits, and economic growth opportunities [11, 12].

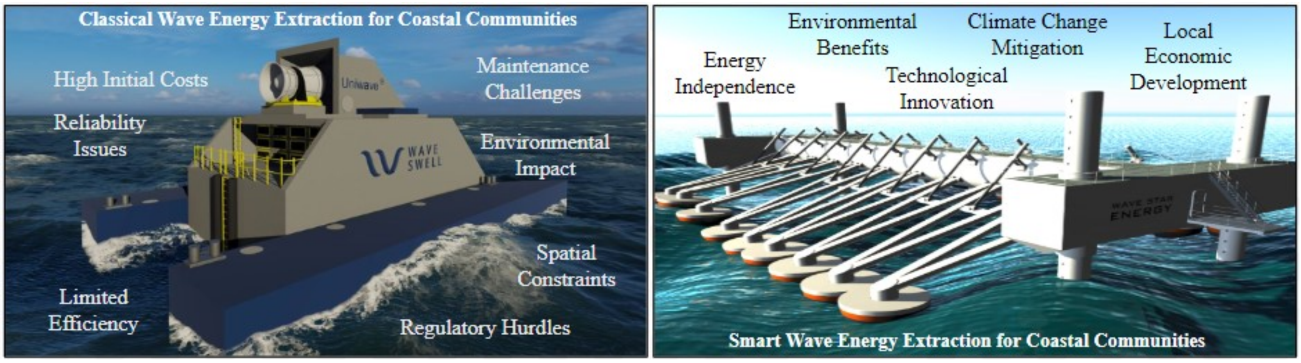

Fig. 2. Comparison between Classical and Smart Wave Energy Extraction in Coastal Communities [11, 12]

Classical grid technologies, as shown in Figure 3, encounter limitations such as cybersecurity risks and high costs. In contrast, smart grids enable real-time monitoring, improved reliability, and better integration of renewable energy and electric vehicles, providing environmental and economic advantages [13, 14].

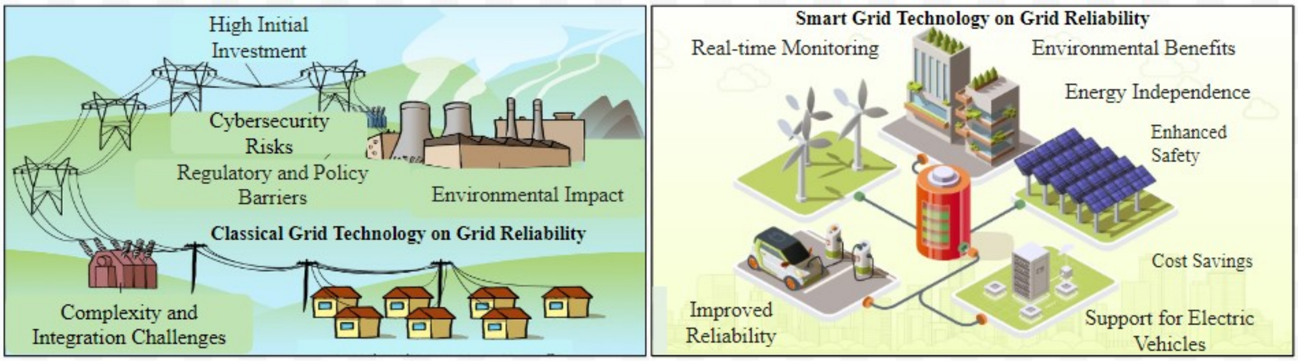

Fig. 3. Comparison between Classical and Smart Grid Technology in Grid Reliability [13, 14]

Innovative sustainable energy systems surpass classical approaches by addressing grid integration issues and climate resilience. Figure 4 highlights these advancements, showcasing the comprehensive benefits of innovative technologies in sustainable energy [15, 16].

Fig. 4. Comparison between Classical and Innovative Sustainable Energy in Power and Energy Domains [15, 16]

With abundant renewable energy options such as solar, wind, hydroelectric power, and biomass, factors like cost, efficiency, and environmental impact must be carefully evaluated. This study employs Multi-Criteria Decision Making (MCDM) approaches to optimize energy systems while integrating Yager's t-norm and t-conorm operators, power aggregation, and prioritized operators. The Complex q-Rung Picture Fuzzy Set (Cq-RPFS) framework further enhances decision-making under uncertainty, making it an ideal tool for energy sector transformation.

Previous research has highlighted the rationale for using Cq-RPFSs. Fathima et al. [17] investigated decision-making in complex q-rung picture fuzzy environments, drawing inspiration from Metacritic, a platform that aggregates public opinions across a spectrum of preferences, from extreme (positive and negative) to intermediate (mixed), in a two-dimensional format (Dimension 1: Metascore, Dimension 2: User Score) as shown in Figure 3 [17]. They referenced Rotten Tomatoes (https:

//www.rottentomatoes.com), which similarly uses a two-dimensional evaluation system (Dimension 1: Tomatometer, Dimension 2: Audience Score) as illustrated in Figure 4 [18]. The evaluation methods of both platforms align closely with the complex q-rung picture fuzzy environment. This leads Fathima et al. [19, 20] to propose the Complex q-Rung Picture Fuzzy Set (Cq-RPFS) as an ideal model for these scenarios. Building on this, Petchimuthu et al. explored the use of Cq-RPFSs in addressing challenges in environmental and resource management. Their work emphasizes the effectiveness of these models in optimizing decision-making processes and developing strategies for complex, real-world problems under uncertainty, such as greenhouse gas emission reduction and water resource management.

In summary, recognizing the need for efficient power and energy management in developing nations, our research focuses on the role of MCDM, Yager's operators, generalized power prioritized aggregation, and complex q-rung picture fuzzy sets in transforming the energy sector.

1.2 *Literature Review*

The traditional framework of set theory struggles to encapsulate the nuances of uncertainty effectively. In a bid to overcome this inherent limitation, Zadeh [21] introduced the concept of fuzzy sets (FS) back in 1965, revolutionizing our ability to handle ambiguity. By introducing a membership value (μ) bounded within $0 \leqslant \mu \leqslant 1$, Zadeh laid the foundation for a more flexible approach to set theory. Building upon this innovation, Atanassov [22] expanded the horizon with intuitionistic fuzzy sets (IFS), enriching the domain with a non-membership value (ξ) alongside the membership value (μ), constrained by $0 \leqslant \mu + \xi \leqslant 1$. The evolution didn't stop there. In 2013, Yager [23] propelled the field forward by introducing Pythagorean fuzzy sets (PyFS), relaxing the constraints of IFS to $\mu^2 + \xi^2 \leqslant 1$, thus enabling a broader spectrum of representation. This momentum continued in 2016 when Yager [24] extended PyFS into the q-rung ortho-pair fuzzy set (q-ROFS), broadening the scope with $\mu^q + \xi^q \leqslant 1$, $q \geqslant 1$. Concurrently, Cuong et al. [25] innovated with picture fuzzy sets (PFS), introducing a neutral value (ν) to bridge the gap between membership (μ) and non-membership (ξ) values, embodying the principle $0 \leqslant \mu+\nu+\xi \leqslant 1$. This dynamic framework allowed for the nuanced expression of uncertainty, capturing the elusive "maybe" alongside the binary extremes of "yes" and "no". The journey of innovation persisted. In 2019, Cuong [26] elevated PFS to new heights with Pythagorean picture fuzzy sets (PyPFS), expanding the boundaries to $\mu^2 + \nu^2 + \xi^2 \leqslant 1$. A year earlier, Li et al. [27] ventured into q-rung picture fuzzy sets (q-RPFS), pushing the envelope further with $\mu^q + \nu^q + \xi^q \leqslant 1$, $q \geqslant 1$. Yet, despite these remarkable strides, the realm of mathematical modeling yearned for a more comprehensive portrayal of vague information. Enter Ramot et al. [28] in a blaze of innovation, introducing complex fuzzy sets (CFS) in 2020. By harnessing the complex-valued membership value $\mu e^{i2\pi\alpha}$ from the unit disk of the complex plane, Ramot's framework encapsulated both amplitude (μ) and phase (α) within the range of 0 to 1, thereby transcending the confines of traditional set theory. The evolution didn't halt there. In 2012, Alkouri et al. [29] further expanded the horizon with complex intuitionistic fuzzy sets (CIFS), delving into the realm of complex-valued non-membership value ($\xi e^{i2\pi\gamma}$) alongside complex-valued membership value ($\mu e^{i2\pi\alpha}$). In 2020, Ullah et al. [30] introduced the complex Pythagorean fuzzy set (CPyFS), broadening the spectrum with $\mu^2 + \xi^2, \alpha^2 + \gamma^2 \leqslant 1$. The journey culminated in 2020 when Liu et al. [31] unveiled the complex q-rung orthopair fuzzy set (Cq-ROFS), pushing the boundaries with $\mu^q + \xi^q, \xi^q + \gamma^q \leqslant 1$, $q \geqslant 1$.

Amidst breathtaking advancements in fuzzy logic and its applications, several pivotal innovations have emerged over the years. Notably, Akram et al. [32] extended CIFS into Complex Picture Fuzzy Sets (CPFS) in 2020 by introducing a complex-valued neutral value ($\nu e^{i2\pi\beta}$) between complex-valued membership ($\mu e^{i2\pi\alpha}$) and non-membership ($\xi e^{i2\pi\gamma}$) values. This framework adhered to the principle $\mu + \nu + \xi, \alpha + \beta + \gamma \leqslant 1$, enabling a more comprehensive representation of uncertainty. Later in 2021, Akram et al. [33] advanced CPFS further into Complex q-Rung Picture Fuzzy Sets (Cq-RPFS), incorporating the flexibility of q-parameters with $\mu^q + \nu^q + \xi^q, \alpha^q + \beta^q + \gamma^q \leqslant 1, q \geqslant 1$. These developments demonstrated an unwavering pursuit of nuanced uncertainty modeling for real-world applications.

Fuzzy sets and their extensions have since found widespread applications in various domains. For instance, Dager et al. [34] utilized Intuitionistic Fuzzy Sets (IFS) in 2024 for decision-making in electrical power plants. Mao et al. [35] applied Pythagorean Fuzzy Sets (PyFS) for photovoltaic power station site selection in 2024. Similarly, Ünver et al. [36] and Mishra et al. [37] employed q-Rung Orthopair Fuzzy Sets (q-ROFS) in 2024 for selecting green technologies and electric vehicle charging station sites, respectively. Senapati et al. [38] demonstrated the application of Picture Fuzzy Sets (PFS) for air-conditioning system selection in 2022, while Dhumras et al. [39] highlighted q-Rung Picture Fuzzy Sets (q-RPFS) in the energy sector in 2024. Complementing these efforts, Hussain et al. [40] utilized Complex Fuzzy Sets (CFS) for electric car assessments in 2023, and Liu et al. [41] employed Complex Intuitionistic Fuzzy Sets (CIFS) for green supply chain management in 2023.

In terms of Aggregation Operators (AOs), Yager et al. [23] seminal work in 1994 introduced the Yager Weighted Aggregation Operator, a cornerstone for integrating data from diverse sources. This operator, including its t-norm variant, has played a crucial role in managing uncertain data. Applications of Yager operators span various fuzzy set environments. For example, Kamal et al. [42] employed Yager operators in q-ROFS in 2024, Liu et al. [43] applied them to q-RPFS in 2020, and Javeed et al. [44] implemented them for Complex q-Rung Orthopair Fuzzy Sets (Cq-ROFS) in 2024. Additionally, Wang et al. [45] leveraged geometric and Heronian averages with generalized Intuitionistic Fuzzy Sets (GIFS) in 2024.

Building on this, the Power Average (PA) operator, introduced by Yager [46] in 2001, emerged as an effective method to incorporate interrelationships among inputs, reducing the impact of biased data. Recent advancements include Jana et al. [47] applying PA operators in PyFS for hybrid aggregation in 2023, Ma et al. [48] utilizing power Bonferroni means in PFS in 2024, and Dhankhar et al. [49] employing geometric power aggregation in q-ROFS in 2023. Similarly, Liu et al. [50] applied power-based operators for ordered aggregation in CIFS in 2024.

Lastly, Yager [51] prioritized AOs, introduced in 2008, have also seen extensive adoption. These operators consider priority relationships during aggregation. Recent examples include Kumar et al. [52] utilizing them in q-ROFS in 2024, Neelam et al. [53] applying them in Lq-ROFS in 2024, and Garg et al. [54] employing them in CIFS in 2023. Additionally, Petchimuthu et al. [18] leveraged prioritized ordered geometric averaging in Cq-RPFS in 2024. Collectively, these advancements underscore the adaptability and importance of aggregation techniques in tackling complex decision-making challenges across industries.

We have identified the following research gap through a comprehensive literature review (Subsection 1.3).

1.3 Research Gap

MCDM techniques are crucial for solving complex, real-world problems, particularly when dealing with uncertain and imprecise information. While advancements in Complex q-Rung Picture Fuzzy Sets (Cq-RPFS) have improved the representation of such information, their integration with sophisticated aggregation operators remains underexplored. Specifically, the literature lacks the application of advanced aggregation operators, such as Yager's PA [46] AOs and Yager's prioritized AOs [51], within the Cq-RPFS framework. This gap limits the ability to address complex decision-making scenarios that involve multiple criteria with varying levels of importance and interdependence. Furthermore, there is a critical absence of studies focusing on the application of these advanced MCDM methodologies to pressing issues like the challenges faced by India's Power and Energy Sector in 2024, particularly in optimizing energy management, reducing inefficiencies, and supporting sustainable development. Existing approaches often fail to account for the complexity and uncertainties inherent in such multi-faceted decision-making processes.

This research seeks to fill these gaps by developing a novel MCDM framework that integrates advanced aggregation operators within the Cq-RPFS environment, specifically designed to optimize decision-making in the context of India's Power and Energy Sector. The framework will leverage innovative techniques for more robust and comprehensive analysis, addressing the sector's challenges and improving its sustainability. The main contributions of this study are:

1.4 Key Contributions of the Proposed Study

The primary contributions of the study are outlined below. Please consult Figure 5 for a visual representation of these key contributions.

(1) Introduction of Yeager's operations, including addition and multiplication between two complex q-rung picture fuzzy numbers (Cq-RPFNs) and scalar product and scalar power operations involving complex q-rung picture fuzzy numbers.

(2) Development of two aggregation operators: the Complex q-rung Picture Fuzzy Generalized Power Prioritized Yager Weighted Average and the Complex q-rung Picture Fuzzy Generalized Power Prioritized Yager Weighted Geometric, within a complex q-rung picture fuzzy set environment.

(3) Exploration of key properties of the proposed operators, including idempotency, monotonicity, and boundedness.

(4) Establishment of a multi-criteria decision-making method utilizing the aggregation operators: the Complex q-rung Picture Fuzzy Generalized Power Prioritized Yager Weighted Average and the Complex q-rung Picture Fuzzy Generalized Power Prioritized Yager Weighted Geometric, within a complex q-rung picture fuzzy set environment.

(5) Comparison of the proposed operators with existing alternatives, highlighting the effectiveness and advantages of the newly developed approaches.

(6) Execution of a case study focusing on India's Power and Energy Sector in 2024.

(7) Demonstration of the efficacy and superiority of the presented approaches through various numerical examples, further validating their practical utility.

Fig. 5. Key Contributions of the Study

The key contributions highlighted above lay a solid foundation for understanding the significance of this research. These contributions address critical gaps and introduce innovative methods that enhance the field.

1.5 Significance of the Proposed Study

This study makes significant contributions in the realm of complex fuzzy data processing and decision-making. First, it introduces Yeager's operations, such as addition, multiplication, scalar product, and scalar power operations involving Cq-RPFNs, expanding the mathematical framework for fuzzy data handling. Second, it develops two novel aggregation operators—Complex q-rung Picture Fuzzy Generalized Power Prioritized Yager Weighted Average (Cq-RPFGPPYWA) and Complex q-rung Picture Fuzzy Generalized Power Prioritized Yager Weighted Geometric (Cq-RPFGPPYWG)—that offer innovative tools for aggregating fuzzy information. The study also explores critical properties like idempotency, monotonicity, and boundedness, ensuring the reliability and consistency of these operators. Furthermore, an MCDM method is established, leveraging these aggregation operators to improve informed decision-making. The proposed operators are compared with existing methods, demonstrating their superior effectiveness. A case study on India's Power and Energy Sector provides real-world application, while numerical examples validate the methods' practicality and robustness.

1.6 *Organization of the Proposed Study*

The paper is structured as follows: **Section 2 (Methodology)** describes the fundamental methodological components essential for implementing the proposed framework. **Section 3 (Results)** This section examines India's power and energy sector through a case study, highlighting the framework's application alongside numerical findings, including the MCDM approach, sensitivity analysis, and comparative analysis. Lastly, **Section 4 (Conclusion)** summarizes the principal findings, examines their implications, notes the study's limitations, and proposes avenues for future research.

2. Methodology

This section introduces key concepts in FS Theory, with a focus on the Cq-RPFS, and explores Yager's t-norm and t-conorm. We also examine Yager's Power Average (POA) and Prioritized Average (PRA) operators. Throughout, unless specified, $\mathscr{X}$ denotes a non-empty set. This foundational overview establishes the theoretical basis for Cq-RPFS and its real-world applications, setting the stage for further analysis in later sections. An illustration of the concepts is provided in Figure 6.

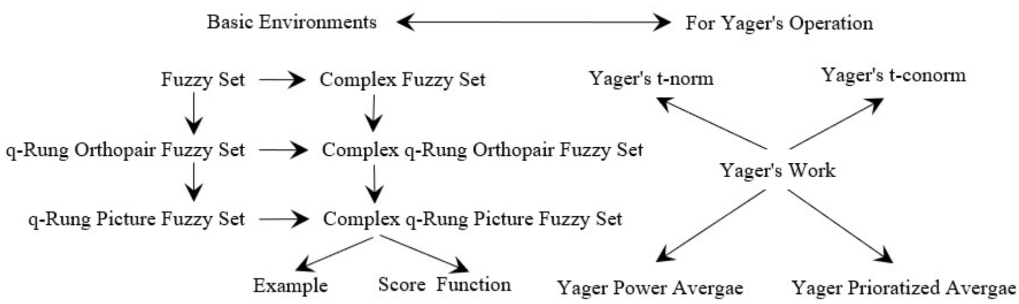

Fig. 6. Illustration of foundational concepts outlined in the preliminaries.

In a pioneering integration of complex fuzzy set theory [28] and q-rung picture fuzzy set [55] models, Akram et al. [33] (2021) introduced a Complex q-rung Picture Fuzzy Set as follows.

Definition 2.1. [33] A Complex q-Rung Picture Fuzzy Set $\mathscr{Y}$ over $\mathscr{X}$ is defined as:

$$\mathscr{Y} = \{(x, \mu(x)e^{i2\pi\alpha(x)}, \nu(x)e^{i2\pi\beta(x)}, \xi(x)e^{i2\pi\gamma(x)}) : x \in \mathscr{X}\}$$

where $\mu(x)e^{i2\pi\alpha(x)}$, $\nu(x)e^{i2\pi\beta(x)}$, and $\xi(x)e^{i2\pi\gamma(x)}$ are complex-valued membership, neutral, and non-membership grade of $x \in \mathscr{X}$ respectively such that $\mu(x), \alpha(x), \nu(x), \beta(x), \xi(x), \gamma(x) \in [0, 1]$. These entities adhere to the q-rung conditions $\mu(x)^q + \nu(x)^q + \xi(x)^q \leqslant 1$ and $\alpha(x)^q + \beta(x)^q + \gamma(x)^q \leqslant 1$, $(q \geqslant 1)$. The Complex q-Rung Picture Fuzzy Number (Cq-RPFN), $\mathscr{Y}$, or its variant $\mathscr{Y}_k$

$(k = 1, 2, \ldots)$, is expressed as $\mathscr{Y} = \langle(\mu, \alpha), (\nu, \beta), (\xi, \gamma)\rangle$ or $\mathscr{Y}_k = \langle(\mu_k, \alpha_k), (\nu_k, \beta_k), (\xi_k, \gamma_k)\rangle$ respectively.

Akram et al. [33] introduced a score function for any Cq-RPFN, $\mathscr{Y} = \langle(\mu, \alpha), (\nu, \beta), (\xi, \gamma)\rangle$, defined by $\mathcal{S}(\mathscr{Y}) = (\mu^q - \nu^q - \xi^q) + (\frac{\alpha}{2\pi})^q - (\frac{\beta}{2\pi})^q - (\frac{\gamma}{2\pi})^q)$, $(q \geqslant 1)$. The resulting value of $\mathcal{S}(\mathscr{Y})$ may fall within the interval $[-2, 2]$. To ensure that $\mathcal{S}(\mathscr{Y})$ lies within the more convenient interval $[0, 1]$ for ease of computation, we have made a slight modification to Akram et al. [33] score function for Cq-RPFN as follows.

Definition 2.2. For any Cq-RPFN ($q \geqslant 1$) denoted by $\mathscr{Y} = \langle(\mu, \alpha), (\nu, \beta), (\xi, \gamma)\rangle$, the score function is defined as:

$$\mathcal{S}(\mathscr{Y}) = \frac{1}{2} + \frac{1}{6}(\mu^q + \alpha^q - \nu^q - \beta^q - \xi^q - \gamma^q) \in [0, 1] \tag{2.1}$$

The definition of the relationship between the score of Cq-RPFN is provided in Definition 2.3.

Definition 2.3. [33] For any two Cq-RPFNs, denoted as $\mathscr{Y}_1$ and $\mathscr{Y}_2$, the relationship between scores of $\mathscr{Y}_1$ and $\mathscr{Y}_2$ is defined as follows:

$$\begin{aligned}
&\text{If } \mathcal{S}(\mathscr{Y}_1) < \mathcal{S}(\mathscr{Y}_2) \Rightarrow \mathscr{Y}_1 < \mathscr{Y}_2 \\
&\text{If } \mathcal{S}(\mathscr{Y}_1) > \mathcal{S}(\mathscr{Y}_2) \Rightarrow \mathscr{Y}_1 > \mathscr{Y}_2 \\
&\text{If } \mathcal{S}(\mathscr{Y}_1) = \mathcal{S}(\mathscr{Y}_2) \Rightarrow \mathscr{Y}_1 = \mathscr{Y}_2
\end{aligned}$$

In the following Definition 2.4, we formulated a distance measure, denoted as $\mathscr{D}$, between two Cq-RPFNs $\mathscr{Y}_i$ and $\mathscr{Y}_k$. This measure considers differences in the components μ^q, α^q, ν^q, β^q, ξ^q, and γ^q weighted equally with a scaling factor of $\frac{1}{6}$. The distance measure presented in Equation 2.2 draws inspiration from the Minkowski distance widely used in literature for comparing vectors in multidimensional space [56]. However, our formulation is uniquely tailored to the characteristics of Cq-RPFNs, encompassing both state and action components in a cohesive and specialized manner.

Definition 2.4. For Cq-RPFNs, $\mathscr{Y}_i = \langle(\mu_i, \alpha_i), (\nu_i, \beta_i), (\xi_i, \gamma_i)\rangle$ and $\mathscr{Y}_k = \langle(\mu_k, \alpha_k), (\nu_k, \beta_k), (\xi_k, \gamma_k)\rangle$ (where i and k are fixed positive integers), the distance measure between $\mathscr{Y}_i$ and $\mathscr{Y}_k$ is defined as

$$\mathscr{D}(\mathscr{Y}_i, \mathscr{Y}_k) = \frac{1}{6}(|{\mu_i}^q - {\mu_k}^q| + |{\alpha_i}^q - {\alpha_k}^q| + |{\nu_i}^q - {\nu_k}^q| + |{\beta_i}^q - {\beta_k}^q| + |{\xi_i}^q - {\xi_k}^q| + |{\gamma_i}^q - {\gamma_k}^q|) \tag{2.2}$$

In Definition 2.5, Yager's t-norm (YTN) and t-conorm (YTCN) are defined as binary operations for values in the interval $[0, 1]$, introducing aggregation functions that consider the influence of a parameter λ in combining inputs. YTN aggregates by taking the minimum, while YTCN combines inputs through 1−minimization, both influenced by the λ parameter.

Definition 2.5. [23] The YTN and YTCN for any two $x, y \in [0, 1]$, and $\lambda \in (0, \infty)$ are defined as follows.

$$\text{YTN}(x, y) = \min(1, (x^\lambda + y^\lambda)^{1/\lambda})$$

$$\text{YTCN}(x, y) = 1 - \min(1, ((1 - x)^\lambda + (1 - y)^\lambda)^{1/\lambda})$$

The Power Average (PA) operator, introduced by Yager [46], revolutionizes decision-making by meticulously accounting for data interrelationships, thus fostering objectivity. Its inception has catalyzed scholarly exploration in aggregation theory.

Definition 2.6. [46] Let's consider a set of criteria $\mathscr{Y}_i$ for $i = 1, 2, \ldots, m$. The Power Average (POA) Operator is defined as:

$$\text{POA}(\mathscr{Y}_1, \mathscr{Y}_2, \ldots, \mathscr{Y}_m) = \oplus_{i=1}^{m} \Theta_i \mathscr{Y}_i,$$

where the Power coefficients Θ_i are calculated as:

$$\Theta_i = \frac{1 + \mathscr{S}_i}{\sum_{k=1}^{m}(1 + \mathscr{S}_k)},$$

and $\mathscr{S}_i = \sum_{\substack{k=1 \\ k \neq i}}^{m} [1 - |\mathscr{Y}_i - \mathscr{Y}_k|]$ for $i = 1, 2, \ldots, m$.

Yager [51] exploration delves into Prioritized Average (PRA), presenting a systematic method to integrate priority levels for refined decision-making processes.

Definition 2.7. [51] Let's consider a set of criteria $\mathscr{Y}_i$ for $i = 1, 2, \ldots, m$. The Prioritized Average (PRA) Operator is defined as:

$$\text{PRA}(\mathscr{Y}_1, \mathscr{Y}_2, \ldots, \mathscr{Y}_m) = \oplus_{i=1}^{m} \Theta_i \mathscr{Y}_i,$$

where the Prioritized coefficients Θ_i are calculated as:

$$\Theta_i = \frac{\mathscr{T}_i}{\sum_{k=1}^{m} \mathscr{T}_k},$$

with $\mathscr{T}_1 = 1$ and $\mathscr{T}_i = \prod_{k=1}^{i-1} \mathcal{S}(\mathscr{Y}_k)$ $(i = 2, \ldots, m)$.

2.1 *Operations of Yager on Complex q-Rung Picture Fuzzy Numbers*

This subsection delves into Yager operations, specifically addition, multiplication, and scalar manipulation, as applied to Cq-RPFNs with the use of YTN and YTCN (Definition 2.5). We present examples demonstrating these operations, concentrating on their main characteristics without including detailed proofs.

Definition 2.8. The Yager operations $\oplus$ and $\otimes$ between two Cq-RPFNs, $\mathscr{Y}_1 = \langle(\mu_1, \alpha_1), (\nu_1, \beta_1), (\xi_1, \gamma_1)\rangle$ and $\mathscr{Y}_2 = \langle(\mu_2, \alpha_2), (\nu_2, \beta_2), (\xi_2, \gamma_2)\rangle$, with $\rho > 0$, $\lambda \in (0, \infty)$, are defined as follows:

$$\mathscr{Y}_1 \oplus \mathscr{Y}_2 = \left\langle \begin{array}{c} \left(\left[1 - \min\{1, ((1 - \mu_1{}^q)^\lambda + (1 - \mu_2{}^q)^\lambda)^{1/\lambda}\}\right]^{1/q}, \left[1 - \min\{1, ((1 - \alpha_1{}^q)^\lambda + (1 - \alpha_2{}^q)^\lambda)^{1/\lambda}\}\right]^{1/q}\right), \\ \left(\left[\min\{1, (\nu_1^{q\lambda} + \nu_2^{q\lambda})^{1/\lambda}\}\right]^{1/q}, \left[\min\{1, (\beta_1^{q\lambda} + \beta_2^{q\lambda})^{1/\lambda}\}\right]^{1/q}\right), \\ \left(\left[\min\{1, (\xi_1^{q\lambda} + \xi_2^{q\lambda})^{1/\lambda}\}\right]^{1/q}, \left[\min\{1, (\gamma_1^{q\lambda} + \gamma_2^{q\lambda})^{1/\lambda}\}\right]^{1/q}\right) \end{array} \right\rangle \tag{2.3}$$

$$\mathscr{Y}_1 \otimes \mathscr{Y}_2 = \left\langle \begin{array}{c} \left(\left[\min\{1, (\mu_1^{q\lambda} + \mu_2^{q\lambda})^{1/\lambda}\}\right]^{1/q}, \left[\min\{1, (\alpha_1^{q\lambda} + \alpha_2^{q\lambda})^{1/\lambda}\}\right]^{1/q}\right), \\ \left(\left[1 - \min\{1, ((1 - \nu_1{}^q)^\lambda + (1 - \nu_2{}^q)^\lambda)^{1/\lambda}\}\right]^{1/q}, \left[1 - \min\{1, ((1 - \beta_1{}^q)^\lambda + (1 - \beta_2{}^q)^\lambda)^{1/\lambda}\}\right]^{1/q}\right), \\ \left(\left[1 - \min\{1, ((1 - \xi_1{}^q)^\lambda + (1 - \xi_2{}^q)^\lambda)^{1/\lambda}\}\right]^{1/q}, \left[1 - \min\{1, ((1 - \gamma_1{}^q)^\lambda + (1 - \gamma_2{}^q)^\lambda)^{1/\lambda}\}\right]^{1/q}\right) \end{array} \right\rangle \tag{2.4}$$

$$\rho\mathscr{Y}_1 = \left\langle \begin{array}{c} \left(\left[1 - \min\{1, (\rho(1 - \mu_1{}^q)^\lambda)^{1/\lambda}\}\right]^{1/q}, \left[1 - \min\{1, (\rho(1 - \alpha_1{}^q)^\lambda)^{1/\lambda}\}\right]^{1/q}\right), \\ \left(\left[\min\{1, (\rho\nu_1^{q\lambda})^{1/\lambda}\}\right]^{1/q}, \left[\min\{1, (\rho\beta_1^{q\lambda})^{1/\lambda}\}\right]^{1/q}\right), \\ \left(\left[\min\{1, (\rho\xi_1^{q\lambda})^{1/\lambda}\}\right]^{1/q}, \left[\min\{1, (\rho\gamma_1^{q\lambda})^{1/\lambda}\}\right]^{1/q}\right) \end{array} \right\rangle \tag{2.5}$$

$$\mathscr{Y}_1^{\rho} = \left\langle \begin{array}{c} \left(\left[\min\{1,(\rho\mu_1^{q\lambda})^{1/\lambda}\}\right]^{1/q}, \left[\min\{1,(\rho\alpha_1^{q\lambda})^{1/\lambda}\}\right]^{1/q}\right), \\ \left(\left[1-\min\{1,(\rho(1-\nu_1{}^q)^\lambda)^{1/\lambda}\}\right]^{1/q}, \left[1-\min\{1,(\rho(1-\beta_1{}^q)^\lambda)^{1/\lambda}\}\right]^{1/q}\right), \\ \left(\left[1-\min\{1,(\rho(1-\xi_1{}^q)^\lambda)^{1/\lambda}\}\right]^{1/q}, \left[1-\min\{1,(\rho(1-\gamma_1{}^q)^\lambda)^{1/\lambda}\}\right]^{1/q}\right) \end{array} \right\rangle \tag{2.6}$$

To exemplify Yager's operations as defined in Equations (2.3), (2.4), (2.5), and (2.6), we examine the details presented in Example 2.1.

Example 2.1. We consider three Cq-RPFNs given by: $\mathscr{Y}_1 = \langle(0.9, 0.15), (0.7, 0.2), (0.9, 0.1)\rangle$, $\mathscr{Y}_2 = \langle(0.8, 0.3),$
$(0.9, 0.6), (0.6, 0.1)\rangle$. Assuming the q-rung criterion as outlined in Definition 2.1 is maintained with $q = 5$ and $\lambda = 2$, we utilize Yager's operations, beginning with the operation $\mathscr{Y}_1 \oplus \mathscr{Y}_2$ as specified in Equation (2.3).

The Yager operation $\oplus$ for the fuzzy sets is computed as follows:

$$\mathscr{Y}_1 \oplus \mathscr{Y}_2 = \langle(\mu, \alpha), (\nu, \beta), (\xi, \gamma)\rangle \tag{2.7}$$

$$\mu = \left[1 - \min\left(1, \left((1-\mu_1^q)^\lambda + (1-\mu_2^q)^\lambda\right)^{1/\lambda}\right)\right]^{1/q}$$

Substituting the values from $\mathscr{Y}_1$ and $\mathscr{Y}_2$, along with $q = 5$ and $\lambda = 2$, we obtain:

$$\mu = 0.733815.$$

Similarly, the remaining parameters $\alpha, \nu, \beta, \xi, \gamma$ using Equation (2.7) are calculated in a similar manner, yielding the final result for $\mathscr{Y}_1 \oplus \mathscr{Y}_2$:

$$\mathscr{Y}_1 \oplus \mathscr{Y}_2 = \langle(0.7338155, 0), (0.9135759, 0.6000095), (0.9015487, 0.1071773)\rangle$$

We also compute the Yager operation $\mathscr{Y}_1 \otimes \mathscr{Y}_2$ in Equation (2.4):

$$\mathscr{Y}_1 \otimes \mathscr{Y}_2 = \langle(0.9244885, 0.3000293), (0.6693109, 0), (0, 0)\rangle$$

Finally, the score function (2.1) is applied to both $\mathscr{Y}_1 \oplus \mathscr{Y}_2$ and $\mathscr{Y}_1 \otimes \mathscr{Y}_2$, resulting in evaluation scores:

$$\text{Score for } \mathscr{Y}_1 \oplus \mathscr{Y}_2 = 0.416345841, \quad \text{Score for } \mathscr{Y}_1 \otimes \mathscr{Y}_2 = 0.884607857$$

These scores represent the evaluation of the on Yager's operations.

Let's consider the fundamental properties of the Yager operations $\oplus$ and $\otimes$, alongside scalar multiplication and scalar power, as delineated in Theorem 2.1.

Theorem 2.1. Let $\mathscr{Y}_1$ and $\mathscr{Y}_2$ denote two Cq-RPFNs, where $\mathscr{Y}_1 = \langle(\mu_1, \alpha_1), (\nu_1, \beta_1), (\xi_1, \gamma_1)\rangle$ and $\mathscr{Y}_2 = \langle(\mu_2, \alpha_2), (\nu_2, \beta_2), (\xi_2, \gamma_2)\rangle$. For any $\rho_1, \rho_2 > 0$, the following conditions hold.

(1) $\mathscr{Y}_1 \oplus \mathscr{Y}_2 = \mathscr{Y}_2 \oplus \mathscr{Y}_1$.

(2) $\mathscr{Y}_1 \otimes \mathscr{Y}_2 = \mathscr{Y}_2 \otimes \mathscr{Y}_1$.

(3) $\rho_1(\mathscr{Y}_1 \oplus \mathscr{Y}_2) = \rho_1\mathscr{Y}_1 \oplus \rho_1\mathscr{Y}_2$.

(4) $(\rho_1 + \rho_2)\mathscr{Y}_1 = \rho_1\mathscr{Y}_1 \oplus \rho_2\mathscr{Y}_1$.

(5) $(\mathscr{Y}_1 \otimes \mathscr{Y}_2)^{\rho_1} = \mathscr{Y}_1^{\rho_1} \otimes \mathscr{Y}_2^{\rho_1}$.

(6) $\mathscr{Y}_1^{\rho_1} \otimes \mathscr{Y}_1^{\rho_2} = \mathscr{Y}_1^{\rho_1+\rho_2}$.

Proof. The proof is easily shown by applying Definition 2.8. □

2.2 The Complex q-rung Picture Fuzzy Generalized Power Prioritized Yager Weighted Average and Geometric Aggregation Operators and Its Distinctive Features

This segment presents two innovative aggregation operators, namely the Cq-RPFGPPYWA and the Cq-RPFGPPYWG, designed specifically for aggregating Cq-RPFNs. Additionally, we delve into their fundamental properties. Let $\mathscr{Y}_i = \langle(\mu_i, \alpha_i), (\nu_i, \beta_i), (\xi_i, \gamma_i)\rangle$ represent the Cq-RPFNs, with $i = 1, 2, \ldots, m$, and let $\rho = [\rho_1, \rho_2, \ldots, \rho_m]$ be the weight vector associated with the Cq-RPFNs $\mathscr{Y}_i$, where $\rho_i > 0$ and $\sum_{i=1}^{m} \rho_i = 1$ unless stated otherwise. To elucidate the aggregation operators, Cq-RPFGPPYWA and Cq-RPFGPPYWG, we initially define the power, prioritized, and generalized power prioritized weighting coefficients as outlined in Definitions 2.9, 2.10, and 2.11, respectively.

Definition 2.9. The power weighting coefficients, represented by $\mathscr{S}_i$, are defined for Cq-RPFN, denoted as $\mathscr{Y}_i$ $(i = 1, 2, \ldots, m)$, in the following manner.

$$\mathscr{S}_i = \sum_{\substack{k=1 \\ k\neq i}}^{m} \left[1 - \mathscr{D}(\mathscr{Y}_i, \mathscr{Y}_k)\right], \tag{2.8}$$

where $\mathscr{D}(\mathscr{Y}_i, \mathscr{Y}_k)$ is the distance measure between $\mathscr{Y}_i$ and $\mathscr{Y}_k$ as defined in Equation (2.2).

Definition 2.10. The prioritized weighting coefficients, represented by $\mathscr{T}_i$, are defined for Cq-RPFN, denoted as $\mathscr{Y}_i$ $(i = 1, 2, \ldots, m)$, in the following manner.

$$\mathscr{T}_1 = 1, \tag{2.9}$$

$$\mathscr{T}_i = \prod_{k=1}^{i-1} \mathcal{S}(\mathscr{Y}_k), \quad i = 2, \ldots, m. \tag{2.10}$$

where $\mathcal{S}(\mathscr{Y}_k)$ is the score function as defined in Equation (2.1).

Definition 2.11. The Generalized Power Prioritized Weighting Coefficients, represented by Θ_i, are defined for Cq-RPFN, denoted as $\mathscr{Y}_i$ $(i = 1, 2, \ldots, m)$, in the following manner.

$$\Theta_i = \frac{\rho_i \left[u(1 + \mathscr{S}_i) + v\mathscr{T}_i\right]}{\sum_{k=1}^{m} \rho_k \left[u(1 + \mathscr{S}_k) + v\mathscr{T}_k\right]} \tag{2.11}$$

In this context, the parameters u and v, which range from 0 to 1, can be customized according to particular needs. In the article, unless stated otherwise, the power, prioritized, and generalized power prioritized weighting coefficients, denoted by $\mathscr{S}_i$, $\mathscr{T}_i$, and Θ_i respectively (where $i = 1, 2, \ldots, m$), remain constant.

2.2.1 Investigating the Complex q-rung Picture Fuzzy Generalized Power Prioritized Yager Weighted Average Operator and Its Essential Attributes

This subsection introduces the AOs, Cq-RPFGPPYWA, and a relevant Example, examining their key characteristics like idempotency, boundedness, and monotonicity, along with straightforward proofs to support these properties.

Definition 2.12. The Complex q-rung Picture Fuzzy Generalized Power Prioritized Yager Weighted Average (Cq-RPFGPPYWA) Aggregation Operator is defined as:

$$\text{Cq-RPFGPPYWA}(\mathscr{Y}_1, \mathscr{Y}_2, \ldots, \mathscr{Y}_m) = \oplus_{i=1}^{m} \Theta_i \mathscr{Y}_i,$$

where Θ_i is defined according to Equation (2.11).

When setting $u = 1$ and $v = 0$ in Equation (2.11), the transformed equation, denoted as Equation (2.12), takes the form of the Complex q-rung Picture Fuzzy Power Yager Weighted Average (Cq-RPFPOYWA) Aggregation Operator, as defined in Definition 2.13.

Definition 2.13. The Cq-RPFPOYWA Aggregation Operator is defined as:

$$\text{Cq-RPFPOYWA}(\mathscr{Y}_1, \mathscr{Y}_2, \ldots, \mathscr{Y}_m) = \oplus_{i=1}^{m} \Omega_i \mathscr{Y}_i,$$

where the power weighting coefficients Ω_i are determined by:

$$\Omega_i = \frac{\rho_i (1 + \mathscr{S}_i)}{\sum_{k=1}^{m} \rho_k (1 + \mathscr{S}_k)} \tag{2.12}$$

When substituting $u = 0$ and $v = 1$ into Equation (2.11), the resulting equation, referred to as Equation (2.13), adopts the structure of the Complex q-rung Picture Fuzzy Prioritized Yager Weighted Average (Cq-RPFPRYWA) Aggregation Operator, as defined in Definition 2.14. However, our main focus in this section is exclusively on the Complex q-rung Picture Fuzzy Generalized Power Prioritized Yager Weighted Average (Cq-RPFGPPYWA) Aggregation Operator.

Definition 2.14. The Cq-RPFPRYWA Aggregation Operator is defined as:

$$\text{Cq-RPFPRYWA}(\mathscr{Y}_1, \mathscr{Y}_2, \ldots, \mathscr{Y}_m) = \oplus_{i=1}^{m} \Psi_i \mathscr{Y}_i,$$

where the prioritized weighting coefficients Ψ_i are computed as:

$$\Psi_i = \frac{\rho_i \mathscr{T}_i}{\sum_{k=1}^{m} \rho_k \mathscr{T}_k} \tag{2.13}$$

In Theorem 2.2, we establish that the aggregation of Complex q-rung Picture Fuzzy Numbers (Cq-RPFNs), denoted as $\mathscr{Y}_i$ for $i = 1, 2, \ldots, m$, using the Cq-RPFGPPYWA operator, results in another Cq-RPFN.

Theorem 2.2. The aggregation value of Cq-RPFNs, $\mathscr{Y}_i = \langle (\mu_i, \alpha_i), (\nu_i, \beta_i), (\xi_i, \gamma_i) \rangle$ for $i = 1, 2, \ldots, m$, when applying the Cq-RPFGPPYWA operator, is again a Cq-RPFN. The aggregation is derived as follows:

$$\text{Cq-RPFGPPYWA}(\mathscr{Y}_1, \mathscr{Y}_2, \ldots, \mathscr{Y}_m) = \oplus_{i=1}^{m} \Theta_i \mathscr{Y}_i$$

$$= \left\langle \begin{array}{c} \left(\left[1-\min\{1,(\sum_{i=1}^{m}\Theta_i(1-\mu_i{}^q)^\lambda)^{1/\lambda}\}\right]^{1/q},\left[1-\min\{1,(\sum_{i=1}^{m}\Theta_i(1-\alpha_i{}^q)^\lambda)^{1/\lambda}\}\right]^{1/q}\right), \\ \left(\left[\min\{1,(\sum_{i=1}^{m}\Theta_i\nu_i^{q\lambda})^{1/\lambda}\}\right]^{1/q},\left[\min\{1,(\sum_{i=1}^{m}\Theta_i\beta_i^{q\lambda})^{1/\lambda}\}\right]^{1/q}\right), \\ \left(\left[\min\{1,(\sum_{i=1}^{m}\Theta_i\xi_i^{q\lambda})^{1/\lambda}\}\right]^{1/q},\left[\min\{1,(\sum_{i=1}^{m}\Theta_i\gamma_i^{q\lambda})^{1/\lambda}\}\right]^{1/q}\right) \end{array} \right\rangle \tag{2.14}$$

Proof. Mathematical induction provides a reliable method for verifying the correctness of a proof.

Case 1. Let's assume $m = 2$, and represent the value $\Theta_1\mathscr{Y}_1$ as $\langle(\bar{\mu}_1,\bar{\alpha}_1),(\bar{\nu}_1,\bar{\beta}_1),(\bar{\xi}_1,\bar{\gamma}_1)\rangle$, and $\Theta_2\mathscr{Y}_2$ as $\langle(\bar{\mu}_2,\bar{\alpha}_2),(\bar{\nu}_2,\bar{\beta}_2),(\bar{\xi}_2,\bar{\gamma}_2)\rangle$. Utilizing Equation (2.3), we can then express the subsequent relationship:

$$\text{Cq-RPFGPPYWA}(\mathscr{Y}_1,\mathscr{Y}_2)=\oplus_{i=1}^{2}\Theta_i\mathscr{Y}_i$$

$$= \left\langle \begin{array}{c} \left(\left[1-\min\{1,((1-\bar{\mu}_1{}^q)^\lambda+(1-\bar{\mu}_2{}^q)^\lambda)^{1/\lambda}\}\right]^{1/q},\left[1-\min\{1,((1-\bar{\alpha}_1{}^q)^\lambda+(1-\bar{\alpha}_2{}^q)^\lambda)^{1/\lambda}\}\right]^{1/q}\right), \\ \left(\left[\min\{1,((\bar{\nu}_1{}^q)^\lambda+(\bar{\nu}_2{}^q)^\lambda)^{1/\lambda}\}\right]^{1/q},\left[\min\{1,((\bar{\beta}_1{}^q)^\lambda+(\bar{\beta}_2{}^q)^\lambda)^{1/\lambda}\}\right]^{1/q}\right), \\ \left(\left[\min\{1,((\bar{\xi}_1{}^q)^\lambda+(\bar{\xi}_2{}^q)^\lambda)^{1/\lambda}\}\right]^{1/q},\left[\min\{1,((\bar{\gamma}_1{}^q)^\lambda+(\bar{\gamma}_2{}^q)^\lambda)^{1/\lambda}\}\right]^{1/q}\right) \end{array} \right\rangle \tag{2.15}$$

It is clear that for every $i = 1, 2$, according to Equation (2.5), the following relationships are valid.

$$\bar{\mathscr{R}}_i = \left[1-\min\{1,(\Theta_i(1-\mathscr{R}_i^q)^\lambda)^{1/\lambda}\}\right]^{1/q} \quad \text{for all} \quad \mathscr{R}=\mu,\alpha$$

$$\bar{\mathscr{R}}_i = \left[\min\{1,(\Theta_i(\mathscr{R}_i^q)^\lambda)^{1/\lambda}\}\right]^{1/q} \quad \text{for all} \quad \mathscr{R}=\nu,\beta,\xi,\gamma$$

By substituting these expressions into Equation 2.15, we derive the modified form of Equation 2.15.

$$\text{Cq-RPFGPPYWA}(\mathscr{Y}_1,\mathscr{Y}_2)=\oplus_{i=1}^{2}\Theta_i\mathscr{Y}_i$$

$$= \left\langle \begin{array}{c} \left(\left[1-\min\{1,(\sum_{i=1}^{2}\Theta_i(1-\mu_i{}^q)^\lambda)^{1/\lambda}\}\right]^{1/q},\left[1-\min\{1,(\sum_{i=1}^{2}\Theta_i(1-\alpha_i{}^q)^\lambda)^{1/\lambda}\}\right]^{1/q}\right), \\ \left(\left[\min\{1,(\sum_{i=1}^{2}\Theta_i\nu_i^{q\lambda})^{1/\lambda}\}\right]^{1/q},\left[\min\{1,(\sum_{i=1}^{2}\Theta_i\beta_i^{q\lambda})^{1/\lambda}\}\right]^{1/q}\right), \\ \left(\left[\min\{1,(\sum_{i=1}^{2}\Theta_i\xi_i^{q\lambda})^{1/\lambda}\}\right]^{1/q},\left[\min\{1,(\sum_{i=1}^{2}\Theta_i\gamma_i^{q\lambda})^{1/\lambda}\}\right]^{1/q}\right) \end{array} \right\rangle$$

Case 2. If the result holds for $m = p$, then we demonstrate for $m = p+1$. Let's assume $\oplus_{i=1}^{p}\Theta_i\mathscr{Y}_i = \langle(\bar{\mu}_\Delta,\bar{\alpha}_\Delta),(\bar{\nu}_\Delta,\bar{\beta}_\Delta),(\bar{\xi}_\Delta,\bar{\gamma}_\Delta)\rangle$, and $\Theta_{p+1}\mathscr{Y}_{p+1} = \langle(\bar{\mu}_{p+1},\bar{\alpha}_{p+1}),(\bar{\nu}_{p+1},\bar{\beta}_{p+1}),(\bar{\xi}_{p+1},\bar{\gamma}_{p+1})\rangle$. Consequently, utilizing Equation (2.3) yields:

$$\text{Cq-RPFGPPYWA}(\mathscr{Y}_1,\mathscr{Y}_2,\ldots,\mathscr{Y}_p,\mathscr{Y}_{p+1})=\oplus_{i=1}^{p}\Theta_i\mathscr{Y}_i\oplus\Theta_{p+1}\mathscr{Y}_{p+1}$$

$$= \left\langle \begin{array}{c} \left(\left[1-\min\{1,((1-\bar{\mu}_\Delta^q)^\lambda+(1-\bar{\mu}_{p+1}^q)^\lambda)^{1/\lambda}\}\right]^{1/q},\left[1-\min\{1,((1-\bar{\alpha}_\Delta^q)^\lambda+(1-\bar{\alpha}_{p+1}^q)^\lambda)^{1/\lambda}\}\right]^{1/q}\right), \\ \left(\left[\min\{1,((\bar{\nu}_\Delta^q)^\lambda+(\bar{\nu}_{p+1}^q)^\lambda)^{1/\lambda}\}\right]^{1/q},\left[\min\{1,((\bar{\beta}_\Delta^q)^\lambda+(\bar{\beta}_{p+1}^q)^\lambda)^{1/\lambda}\}\right]^{1/q}\right), \\ \left(\left[\min\{1,((\bar{\xi}_\Delta^q)^\lambda+(\bar{\xi}_{p+1}^q)^\lambda)^{1/\lambda}\}\right]^{1/q},\left[\min\{1,((\bar{\gamma}_\Delta^q)^\lambda+(\bar{\gamma}_{p+1}^q)^\lambda)^{1/\lambda}\}\right]^{1/q}\right) \end{array} \right\rangle \tag{2.16}$$

From the assumption, it is evident that we have the following.

$$\bar{\mathscr{R}}_\Delta = \left[1 - \min\{1, (\sum_{i=1}^{p} \Theta_i (1 - \mathscr{R}_i^q)^\lambda)^{1/\lambda}\}\right]^{1/q} \quad \text{for all} \quad \mathscr{R} = \mu, \alpha$$

$$\bar{\mathscr{R}}_\Delta = \left[\min\{1, (\sum_{i=1}^{p} \Theta_i (\mathscr{R}_i^q)^\lambda)^{1/\lambda}\}\right]^{1/q} \quad \text{for all} \quad \mathscr{R} = \nu, \beta, \xi, \gamma$$

Once more, referring to Equation (2.5), we obtain the following.

$$\bar{\mathscr{R}}_{p+1} = \left[1 - \min\{1, (\Theta_{p+1}(1 - \mathscr{R}_{p+1}^q)^\lambda)^{1/\lambda}\}\right]^{1/q} \quad \text{for all} \quad \mathscr{R} = \mu, \alpha$$

$$\bar{\mathscr{R}}_{p+1} = \left[\min\{1, (\Theta_{p+1}(\mathscr{R}_{p+1}^q)^\lambda)^{1/\lambda}\}\right]^{1/q} \quad \text{for all} \quad \mathscr{R} = \nu, \beta, \xi, \gamma$$

If we substitute these values into Equation 2.16, then Equation 2.16 becomes as follows.

$$\text{Cq-RPFGPPYWA}(\mathscr{Y}_1, \mathscr{Y}_2, \ldots, \mathscr{Y}_{p+1}) = \oplus_{i=1}^{p+1} \Theta_i \mathscr{Y}_i$$

$$= \left\langle \begin{array}{c} \left(\left[1 - \min\{1, (\sum_{i=1}^{p+1} \Theta_i (1 - {\mu_i}^q)^\lambda)^{1/\lambda}\}\right]^{1/q}, \left[1 - \min\{1, (\sum_{i=1}^{p+1} \Theta_i (1 - {\alpha_i}^q)^\lambda)^{1/\lambda}\}\right]^{1/q}\right), \\ \left(\left[\min\{1, (\sum_{i=1}^{p+1} \Theta_i {\nu_i^q}^\lambda)^{1/\lambda}\}\right]^{1/q}, \left[\min\{1, (\sum_{i=1}^{p+1} \Theta_i {\beta_i^q}^\lambda)^{1/\lambda}\}\right]^{1/q}\right), \\ \left(\left[\min\{1, (\sum_{i=1}^{p+1} \Theta_i {\xi_i^q}^\lambda)^{1/\lambda}\}\right]^{1/q}, \left[\min\{1, (\sum_{i=1}^{p+1} \Theta_i {\gamma_i^q}^\lambda)^{1/\lambda}\}\right]^{1/q}\right) \end{array} \right\rangle$$

Therefore, the result remains valid for all values of m.

□

Example 2.2 focuses on the aggregation process of three Cq-RPFNs by utilizing the AO, Cq-RPFGPPYWA defined in Equation (2.14) (Theorem 2.2).

Example 2.2. We consider three Cq-RPFNs given by:

$$\mathscr{Y}_1 = \langle(0.8, 0.4), (0.6, 0.3), (0.9, 0.5)\rangle \tag{2.17}$$

$$\mathscr{Y}_2 = \langle(0.7, 0.2), (0.9, 0.7), (0.5, 0.1)\rangle \tag{2.18}$$

$$\mathscr{Y}_3 = \langle(0.6, 0.3), (0.7, 0.5), (0.4, 0.2)\rangle \tag{2.19}$$

The criteria weights are $\rho_1 = 0.2$, $\rho_2 = 0.1$, and $\rho_3 = 0.7$. According to the q-rung conditions specified in Definition 2.1, the q-value for the Cq-RPFNs, $\mathscr{Y}_1$, $\mathscr{Y}_2$, and $\mathscr{Y}_3$, is determined as $q = 5$.

We proceed to aggregate the Cq-RPFNs ($q = 5$), $\mathscr{Y}_1$, $\mathscr{Y}_2$, and $\mathscr{Y}_3$, employing the AOs, Cq-RPFGPPYWA ($\lambda = 2$, $u = 0.8$, $v = 0.2$) as defined in Equation (2.14) (Theorem 2.2). To begin with, we calculate the power weighting coefficient factors $\mathscr{S}_i$ ($i = 1, 2, 3$), as defined in Equation (2.8). Setting $i = 1$ and $m = 3$ in Equation (2.8), we have:

$$\mathscr{S}_1 = \sum_{\substack{k=1 \\ k \neq 1}}^{3} [1 - \mathscr{D}(\mathscr{Y}_1, \mathscr{Y}_k)] = [1 - \mathscr{D}(\mathscr{Y}_1, \mathscr{Y}_2)] + [1 - \mathscr{D}(\mathscr{Y}_1, \mathscr{Y}_3)] \tag{2.20}$$

Here, the distance measure $\mathscr{D}(\mathscr{Y}_1, \mathscr{Y}_2)$ is computed using Equation (2.2):

$$\mathscr{D}(\mathscr{Y}_1, \mathscr{Y}_2) = \frac{1}{6}(|\mu_1^q - \mu_2^q| + |\alpha_1^q - \alpha_2^q| + |\nu_1^q - \nu_2^q| + |\beta_1^q - \beta_2^q| + |\xi_1^q - \xi_2^q| + |\gamma_1^q - \gamma_2^q|) \quad (2.21)$$

By substituting $\mu_1 = 0.8$, $\alpha_1 = 0.4$, $\nu_1 = 0.6$, $\beta_1 = 0.3$, $\xi_1 = 0.9$, and $\gamma_1 = 0.5$ from Equation (2.17), along with the corresponding values of μ_2, α_2, ν_2, β_2, ξ_2, and γ_2 from Equation (2.18), and the parameter $q = 5$ into Equation (2.21), we obtain the distance measure $\mathscr{D}(\mathscr{Y}_1, \mathscr{Y}_2) = 0.23973$. Similarly, we find the distance measure $\mathscr{D}(\mathscr{Y}_1, \mathscr{Y}_3) = 0.1646733$. Substituting these distance measures into Equation (2.20), we determine $\mathscr{S}_1 = 1.595596667$. Employing the same procedure, we compute $\mathscr{S}_2 = 1.6481067$ and $\mathscr{S}_3 = 1.7231633$. Next, we proceed to calculate the prioritized weighting coefficient factors $\mathscr{T}_i$ $(i = 1, 2, 3)$, as outlined in Equation (2.9) and (2.10). We determine $\mathscr{T}_1 = 1$ directly from Equation (2.9). Subsequently, for $i = 2, 3$, we compute $\mathscr{T}_i$ according to the procedure described in Equation (2.10):

$$\mathscr{T}_2 = \prod_{k=1}^{1} \mathcal{S}(\mathscr{Y}_k) = \mathcal{S}(\mathscr{Y}_1) \quad (2.22)$$

$$\mathscr{T}_3 = \prod_{k=1}^{2} \mathcal{S}(\mathscr{Y}_k) = \mathcal{S}(\mathscr{Y}_1)\mathcal{S}(\mathscr{Y}_2) \quad (2.23)$$

Here, we calculate the score value $\mathcal{S}(\mathscr{Y}_1)$ using Equation (2.2):

$$\mathcal{S}(\mathscr{Y}_1) = \frac{1}{2} + \frac{1}{6}(\mu_1^q + \alpha_1^q - \nu_1^q - \beta_1^q - \xi_1^q - \gamma_1^q) \quad (2.24)$$

By substituting $\mu_1 = 0.8$, $\alpha_1 = 0.4$, $\nu_1 = 0.6$, $\beta_1 = 0.3$, $\xi_1 = 0.9$, $\gamma_1 = 0.5$ from Equation (2.17), along with the parameter $q = 5$, into Equation (2.24), we obtain the score value $\mathcal{S}(\mathscr{Y}_1) = 0.4393317$. Similarly, we compute the score value $\mathcal{S}(\mathscr{Y}_2) = 0.396428$. Substituting these score values into Equations (2.22) and (2.23), we derive $\mathscr{T}_2 = 0.4393317$ and $\mathscr{T}_3 = 0.1741635$. Next, we proceed to compute the generalized power prioritized weighting coefficients Θ_i $(i = 1, 2, 3)$, as defined in Equation (2.11). Substituting $i = 1$ and $m = 3$ into Equation (2.11), we obtain:

$$\Theta_1 = \frac{\rho_1 \left[u(1 + \mathscr{S}_1) + v\mathscr{T}_1\right]}{\sum_{k=1}^{3} \rho_k \left[u(1 + \mathscr{S}_k) + v\mathscr{T}_k\right]}, \quad (2.25)$$

Here, the expression $\rho_1 \left[u(1 + \mathscr{S}_1) + v\mathscr{T}_1\right] = (0.2)\left[(0.8)(1 + 1.5955967) + (0.2)(1)\right] = 0.4552954667$. Similarly, we determine $\rho_2 \left[u(1 + \mathscr{S}_2) + v\mathscr{T}_2\right] = 0.2206351667$ and $\rho_3 \left[u(1 + \mathscr{S}_3) + v\mathscr{T}_3\right] = 1.549354$. Substituting these values into Equation (2.25), we calculate $\Theta_1 = 0.2046010$. Similarly, we obtain $\Theta_2 = 0.0991492$ and $\Theta_3 = 0.6962499$. Finally, we can aggregate $\mathscr{Y}_1$, $\mathscr{Y}_2$, and $\mathscr{Y}_3$ using the AO, Cq-RPFGPPYWA (Equation (2.14)) as shown below:

$$\text{Cq-RPFGPPYWA}(\mathscr{Y}_1, \mathscr{Y}_2, \mathscr{Y}_3) = \oplus_{i=1}^{3} \Theta_i \mathscr{Y}_i = \langle(\mu, \alpha), (\nu, \beta), (\xi, \gamma)\rangle \quad (2.26)$$

Here, the value of μ is calculated using Equation (2.14) as follows:

$$\mu = \left[1 - \min\{1, (\Theta_1(1 - \mu_1^q)^\lambda + \Theta_2(1 - \mu_2^q)^\lambda + \Theta_3(1 - \mu_3^q)^\lambda)^{1/\lambda}\}\right]^{1/q} \quad (2.27)$$

Substituting $\mu_1 = 0.8$, $\mu_2 = 0.7$, and $\mu_3 = 0.6$ from Equation (2.17), (2.18), and (2.19) respectively, Θ_i $(i = 1, 2, 3)$ from the above calculation, along with the parameters $q = 5$ and $\lambda = 2$, into Equation 2.27, we find $\mu = 0.6670648$. Similarly, we compute the parameters α, ν, β, ξ, and γ in Equation (2.26) using Equation (2.14) in conjunction with the provided data. Therefore, from Equation (2.26), we obtain the aggregation of Cq-RPFNs, $\mathscr{Y}_1$, $\mathscr{Y}_2$, and $\mathscr{Y}_3$ as follows:

$$\text{Cq-RPFGPPYWA}(\mathscr{Y}_1, \mathscr{Y}_2, \mathscr{Y}_3) = \langle(0.6670, 0.3282), (0.7488, 0.5677), (0.7681, 0.4266)\rangle$$

Theorem 2.3 explores the Idempotency Property of the Cq-RPFGPPYWA aggregation operator within Cq-RPFS.

Theorem 2.3. (Idempotency Property) If $\mathscr{Y}_i = \langle(\mu_i, \alpha_i), (\nu_i, \beta_i), (\xi_i, \gamma_i)\rangle$ for $i = 1, 2, \ldots, m$ such that $\mathscr{Y}_i = \mathscr{Y}$, where $\mathscr{Y} = \langle(\mu, \alpha), (\nu, \beta), (\xi, \gamma)\rangle$, then the aggregation operator Cq-RPFGPPYWA, when applied to $\mathscr{Y}_1, \mathscr{Y}_2, \ldots, \mathscr{Y}_m$, results in $\mathscr{Y}$.

Proof. Given that $\mathscr{R}_i = \mathscr{R}$ for all $\mathscr{R} = \mu, \alpha, \nu, \beta, \xi, \gamma$, Equation (2.14) becomes

$$\text{Cq-RPFGPPYWA}(\mathscr{Y}_1, \mathscr{Y}_2, \ldots, \mathscr{Y}_m) = \oplus_{i=1}^{m}\Theta_i\mathscr{Y}_i$$

$$= \left\langle \begin{array}{c} \left(\left[1-\min\{1, (\sum_{i=1}^{m}\Theta_i(1-\mu^q)^\lambda)^{1/\lambda}\}\right]^{1/q}, \left[1-\min\{1, (\sum_{i=1}^{m}\Theta_i(1-\alpha^q)^\lambda)^{1/\lambda}\}\right]^{1/q}\right), \\ \left(\left[\min\{1, (\sum_{i=1}^{m}\Theta_i\nu^{q\lambda})^{1/\lambda}\}\right]^{1/q}, \left[\min\{1, (\sum_{i=1}^{m}\Theta_i\beta^{q\lambda})^{1/\lambda}\}\right]^{1/q}\right), \\ \left(\left[\min\{1, (\sum_{i=1}^{m}\Theta_i\xi^{q\lambda})^{1/\lambda}\}\right]^{1/q}, \left[\min\{1, (\sum_{i=1}^{m}\Theta_i\gamma^{q\lambda})^{1/\lambda}\}\right]^{1/q}\right) \end{array} \right\rangle \tag{2.28}$$

Because of the condition $\sum_{i=1}^{m}\Theta_i = 1$, the expression in Equation (2.28) becomes $\langle(\mu, \alpha), (\nu, \beta), (\xi, \gamma)\rangle$. Thus,

$$\text{Cq-RPFGPPYWA}(\mathscr{Y}_1, \mathscr{Y}_2, \ldots, \mathscr{Y}_m) = \mathscr{Y}.$$

□

Theorem 2.4 explores the Boundedness Property of the Cq-RPFGPPYWG aggregation operator within Cq-RPFS.

Theorem 2.4. (Boundedness Property) Let $\mathscr{Y}_i = \langle(\mu_i, \alpha_i), (\nu_i, \beta_i), (\xi_i, \gamma_i)\rangle$ $(i = 1, 2, \ldots, m)$ represent the Cq-RPFNs. Assume that

$$\begin{aligned} \mathscr{Y}^- &= \langle(\min_i\{\mu_i\}, \min_i\{\alpha_i\}), (\max_i\{\nu_i\}, \max_i\{\beta_i\}), (\max_i\{\xi_i\}, \max_i\{\gamma_i\})\rangle, \\ \mathscr{Y}^+ &= \langle(\max_i\{\mu_i\}, \max_i\{\alpha_i\}), (\min_i\{\nu_i\}, \min_i\{\beta_i\}), (\min_i\{\xi_i\}, \min_i\{\gamma_i\})\rangle. \end{aligned}$$

We establish the inequality as follows $\mathscr{Y}^- \leqslant \text{Cq-RPFGPPYWA}(\mathscr{Y}_1, \mathscr{Y}_2, \ldots, \mathscr{Y}_m) \leqslant \mathscr{Y}^+$.

Proof. For each index $i = 1, 2, \ldots, m$, the subsequent inequalities are valid

$$\begin{aligned} &\min_i \mathscr{R}_i \leqslant \mathscr{R}_i \leqslant \max_i \mathscr{R}_i \quad \text{for} \quad \mathscr{R} = \mu, \alpha, \\ &\max_i \mathscr{R}_i \geqslant \mathscr{R}_i \geqslant \min_i \mathscr{R}_i \quad \text{for} \quad \mathscr{R} = \nu, \beta, \xi, \gamma. \end{aligned}$$

Consequently, we obtain the following

$$\min_i \mathscr{R} \leqslant \left[1-\min\{1, (\sum_{i=1}^{m}\Theta_i(1-\mathscr{R}_i{}^q)^\lambda)^{1/\lambda}\}\right]^{1/q} \leqslant \max_i \mathscr{R}_i \quad \text{for} \quad \mathfrak{R} = \mu, \alpha,$$

$$\max_i \mathscr{R} \geqslant \left[\min\{1, (\sum_{i=1}^{m}\Theta_i(\mathscr{R}_i{}^q)^\lambda)^{1/\lambda}\}\right]^{1/q} \geqslant \min_i \mathscr{R}_i \quad \text{for} \quad \mathfrak{R} = \nu, \beta, \xi, \gamma$$

This implies that

$$\mathcal{S}(\mathscr{Y}^-) \leqslant \mathcal{S}(\text{Cq-RPFGPPYWA}(\mathscr{Y}_1, \mathscr{Y}_2, \ldots, \mathscr{Y}_m)) \leqslant \mathcal{S}(\mathscr{Y}^+)$$

by Equation (2.1) and Equation (2.14). Thus, the proof is concluded according to Definition 2.3.

□

Theorem 2.5, explores the Monotonicity Property of the Cq-RPFGPPYWG aggregation operator within Cq-RPFS.

Theorem 2.5. (Monotonicity Property) Let $\mathscr{Y}_i = \langle(\mu_i, \alpha_i), (\nu_i, \beta_i), (\xi_i, \gamma_i)\rangle$ for $i = 1, 2, \ldots, m$ and $\mathscr{Y}_i' = \langle(\mu_i', \alpha_i'), (\nu_i', \beta_i'), (\xi_i', \gamma_i')\rangle$ for $i = 1, 2, \ldots, m$ be the Cq-RPFNs. If $\mathscr{Y}_i \leqslant \mathscr{Y}_i'$ for all $i = 1, 2, \ldots, m$, then Cq-RPFGPPYWA$(\mathscr{Y}_1, \mathscr{Y}_2, \ldots, \mathscr{Y}_m) \leqslant$ Cq-RPFGPPYWA$(\mathscr{Y}_1', \mathscr{Y}_2', \ldots, \mathscr{Y}_m')$.

Proof. Assuming $\mathscr{Y}_i \leqslant \mathscr{Y}_i'$ for all $i = 1, 2, \ldots, m$, as per Definition 2.3, we have

$$\mathcal{S}(\mathscr{Y}_i) \leqslant \mathcal{S}(\mathscr{Y}_i') \quad \text{for} \quad i = 1, 2, \ldots, m.$$

Using this, we establish the following inequalities:

$$\mathscr{R}_i \leqslant \mathscr{R}_i' \quad \text{for} \quad \mathscr{R} = \mu, \alpha,$$
$$\mathscr{R}_i \geqslant \mathscr{R}_i' \quad \text{for} \quad \mathscr{R} = \nu, \beta, \xi, \gamma.$$

Consequently, we obtain:

$$\left[1 - \min\{1, (\textstyle\sum_{i=1}^{m} \Theta_i(1 - \mathscr{R}_i{}^q)^\lambda)^{1/\lambda}\}\right]^{1/q} \leqslant$$
$$\left[1 - \min\{1, (\textstyle\sum_{i=1}^{m} \Theta_i(1 - \mathscr{R}_i'^q)^\lambda)^{1/\lambda}\}\right]^{1/q} \quad \text{for} \quad \mathfrak{R} = \mu, \alpha,$$

$$\left[\min\{1, (\textstyle\sum_{i=1}^{m} \Theta_i(\mathscr{R}_i{}^q)^\lambda)^{1/\lambda}\}\right]^{1/q} \geqslant \left[\min\{1, (\textstyle\sum_{i=1}^{m} \Theta_i(\mathscr{R}_i{}^q)^\lambda)^{1/\lambda}\}\right]^{1/q} \quad \text{for} \quad \mathfrak{R} = \nu, \beta, \xi, \gamma.$$

This implies that

$$\mathcal{S}(\text{Cq-RPFGPPYWA}(\mathscr{Y}_1, \mathscr{Y}_2, \ldots, \mathscr{Y}_m)) \leqslant \mathcal{S}(\text{Cq-RPFGPPYWA}(\mathscr{Y}_1', \mathscr{Y}_2', \ldots, \mathscr{Y}_m'))$$

by Equation (2.1) and Equation (2.14). Thus, the proof is concluded by Definition 2.3. ☐

2.2.2 *Investigating the novel Complex q-rung Picture Fuzzy Generalized Power Prioritized Yager Weighted Geometric Aggregation Operator and Its Distinctive Features*

This subsection introduces the AOs, Cq-RPFGPPYWG, and a relevant Example, examining their key characteristics like idempotency, boundedness, and monotonicity, along with straightforward proofs to support these properties.

Definition 2.15. The Complex q-rung Picture Fuzzy Generalized Power Prioritized Yager Weighted Geometric (Cq-RPFGPPYWG) Aggregation Operator is defined as:

$$\text{Cq-RPFGPPYWG}(\mathscr{Y}_1, \mathscr{Y}_2, \ldots, \mathscr{Y}_m) = \otimes_{i=1}^{m} \Theta_i \mathscr{Y}_i,$$

where Θ_i is defined according to Equation (2.11).

When setting $u = 1$ and $v = 0$ in Equation (2.11), the transformed equation, denoted as Equation (2.12), takes the form of the Complex q-rung Picture Fuzzy Power Yager Weighted Geometric (Cq-RPFPOYWG) Aggregation Operator, as defined in Definition 2.16.

Definition 2.16. The Cq-RPFPOYWG Aggregation Operator is defined as:

$$\text{Cq-RPFPOYWG}(\mathscr{Y}_1, \mathscr{Y}_2, \ldots, \mathscr{Y}_m) = \otimes_{i=1}^{m} \Omega_i \mathscr{Y}_i,$$

where Ω_i is defined according to Equation (2.12)

When substituting $u = 0$ and $v = 1$ into Equation (2.11), the resulting equation, referred to as Equation (2.12), adopts the structure of the Complex q-rung Picture Fuzzy Prioritized Yager Weighted Geometric (Cq-RPFPRYWG) Aggregation Operator, as defined in Definition 2.17. However, our main focus in this section is exclusively on the Complex q-rung Picture Fuzzy Generalized Power Prioritized Yager Weighted Geometric (Cq-RPFGPPYWG) Aggregation Operator.

Definition 2.17. The Complex q-rung Picture Fuzzy Prioritized Yager Weighted Geometric (Cq-RPFPRYWG) Aggregation Operator is defined as:

$$\text{Cq-RPFPRYWG}(\mathscr{Y}_1, \mathscr{Y}_2, \ldots, \mathscr{Y}_m) = \otimes_{i=1}^{m} \Psi_i \mathscr{Y}_i,$$

where Ψ_i is defined according to Equation (2.13)

In Theorem 2.6, we establish that the aggregation of Complex q-rung Picture Fuzzy Numbers (Cq-RPFNs), denoted as $\mathscr{Y}_i$ for $i = 1, 2, \ldots, m$, using the Cq-RPFGPPYWG operator, results in another Cq-RPFN.

Theorem 2.6. The aggregation value of Cq-RPFNs, $\mathscr{Y}_i = \langle(\mu_i, \alpha_i), (\nu_i, \beta_i), (\xi_i, \gamma_i)\rangle$ for $i = 1, 2, \ldots, m$, when applying the Cq-RPFGPPYWG operator, is again a Cq-RPFN. The aggregation is derived as follows:

$$\text{Cq-RPFGPPYWG}(\mathscr{Y}_1, \mathscr{Y}_2, \ldots, \mathscr{Y}_m) = \otimes_{i=1}^{m} \Theta_i \mathscr{Y}_i$$

$$= \left\langle \begin{array}{c} \left(\left[\min\{1, (\sum_{i=1}^{m} \Theta_i {\mu_i^q}^\lambda)^{1/\lambda}\}\right]^{1/q}, \left[\min\{1, (\sum_{i=1}^{m} \Theta_i {\alpha_i^q}^\lambda)^{1/\lambda}\}\right]^{1/q} \right), \\ \left(\left[1 - \min\{1, (\sum_{i=1}^{m} \Theta_i (1 - {\nu_i}^q)^\lambda)^{1/\lambda}\}\right]^{1/q}, \left[1 - \min\{1, (\sum_{i=1}^{m} \Theta_i (1 - {\beta_i}^q)^\lambda)^{1/\lambda}\}\right]^{1/q} \right), \\ \left(\left[1 - \min\{1, (\sum_{i=1}^{m} \Theta_i (1 - {\xi_i}^q)^\lambda)^{1/\lambda}\}\right]^{1/q}, \left[1 - \min\{1, (\sum_{i=1}^{m} \Theta_i (1 - {\gamma_i}^q)^\lambda)^{1/\lambda}\}\right]^{1/q} \right) \end{array} \right\rangle \tag{2.29}$$

Proof. We can establish and verify this result by employing a proof methodology similar to the one utilized in Theorem 2.2. □

Example 2.3 focuses on the aggregation process of three Cq-RPFNs by utilizing the AO, Cq-RPFGPPYWG defined in Equation (2.29) (Theorem 2.6).

Example 2.3. Consider the dataset from Example 2.2. We now calculate the aggregation using the Cq-RPFGPPYWG operator:

$$\text{Cq-RPFGPPYWG}(\mathscr{Y}_1, \mathscr{Y}_2, \mathscr{Y}_3) = \otimes_{i=1}^{3} \Theta_i \mathscr{Y}_i = \langle(\mu, \alpha), (\nu, \beta), (\xi, \gamma)\rangle \tag{2.30}$$

Here, the value of μ is determined using the provided data and Equation (2.29):

$$\begin{aligned} \mu &= \left[\min\{1, ((\Theta_1(\mu_1^q)^\lambda + \Theta_2(\mu_2^q)^\lambda + \Theta_3(\mu_3^q)^\lambda)^{1/\lambda}\}\right]^{1/q} \\ &= \left[\min\{1, ((0.20460(0.8^5)^2 + 0.09914(0.7^5)^2 + 0.69624(0.6^5)^2)^{1/2}\}\right]^{1/5} \\ &= 0.7328485. \end{aligned}$$

Similarly, we compute the parameters α, ν, β, ξ, and γ in Equation (2.30) using Equation (2.29) in conjunction with the provided data. Therefore, from Equation (2.30), we obtain the aggregation of Cq-RPFNs, $\mathscr{Y}_1$, $\mathscr{Y}_2$, and $\mathscr{Y}_3$ as follows:

$$\text{Cq-RPFGPPYWG}(\mathscr{Y}_1, \mathscr{Y}_2, \mathscr{Y}_3) = \langle(0.7328485, 0.70953, 0.7199066, 0.4819637, 0.6341494, 0.5400834)\rangle$$

Theorem 2.7 explores the Idempotency Property of the Cq-RPFGPPYWG aggregation operator within Cq-RPFS.

Theorem 2.7. (Idempotency Property) If $\mathscr{Y}_i = \langle(\mu_i, \alpha_i), (\nu_i, \beta_i), (\xi_i, \gamma_i)\rangle$ for $i = 1, 2, \ldots, m$ such that $\mathscr{Y}_i = \mathscr{Y}$, where $\mathscr{Y} = \langle(\mu, \alpha), (\nu, \beta), (\xi, \gamma)\rangle$, then the aggregation operator Cq-RPFGPPYWG, when applied to $\mathscr{Y}_1, \mathscr{Y}_2, \ldots, \mathscr{Y}_m$, results in $\mathscr{Y}$.

Proof. We can establish and verify this result by employing a proof methodology similar to the one utilized in Theorem 2.3. □

Theorem 2.8 explores the Boundedness Property of the Cq-RPFGPPYWG aggregation operator within Cq-RPFS.

Theorem 2.8. (Boundedness Property) Let $\mathscr{Y}_i = \langle(\mu_i, \alpha_i), (\nu_i, \beta_i), (\xi_i, \gamma_i)\rangle$ $(i = 1, 2, \ldots, m)$ represent the Cq-RPFNs. Assume that

$$\mathscr{Y}^- = \langle(\min_i\{\mu_i\}, \min_i\{\alpha_i\}), (\max_i\{\nu_i\}, \max_i\{\beta_i\}), (\max_i\{\xi_i\}, \max_i\{\gamma_i\})\rangle,$$
$$\mathscr{Y}^+ = \langle(\max_i\{\mu_i\}, \max_i\{\alpha_i\}), (\min_i\{\nu_i\}, \min_i\{\beta_i\}), (\min_i\{\xi_i\}, \min_i\{\gamma_i\})\rangle.$$

We establish the inequality as follows $\mathscr{Y}^- \leqslant \text{Cq-RPFGPPYWG}(\mathscr{Y}_1, \mathscr{Y}_2, \ldots, \mathscr{Y}_m) \leqslant \mathscr{Y}^+$.

Proof. We can establish and verify this result by employing a proof methodology similar to the one utilized in Theorem 2.4. □

Theorem 2.9, explores the Monotonicity Property of the Cq-RPFGPPYWG aggregation operator within Cq-RPFS.

Theorem 2.9. (Monotonicity Property) Let $\mathscr{Y}_i = \langle(\mu_i, \alpha_i), (\nu_i, \beta_i), (\xi_i, \gamma_i)\rangle$ for $i = 1, 2, \ldots, m$ and $\mathscr{Y}_i' = \langle(\mu_i', \alpha_i'), (\nu_i', \beta_i'), (\xi_i', \gamma_i')\rangle$ for $i = 1, 2, \ldots, m$ be the Cq-RPFNs. If $\mathscr{Y}_i \leqslant \mathscr{Y}_i'$ for all $i = 1, 2, \ldots, m$, then $\text{Cq-RPFGPPYWG}(\mathscr{Y}_1, \mathscr{Y}_2, \ldots, \mathscr{Y}_m) \leqslant \text{Cq-RPFGPPYWG}(\mathscr{Y}_1', \mathscr{Y}_2', \ldots, \mathscr{Y}_m')$.

Proof. We can establish and verify this result by employing a proof methodology similar to the one utilized in Theorem 2.5. □

2.3 *Methodology for Multi-Criteria Decision Making in Complex q-Rung Picture Fuzzy Environments and Its Practical Application*

We devise a MCDM approach that encompasses identifying alternatives and criteria, assigning weights to each criterion, and employing Cq-RPFNs to assess criteria against alternatives. Subsequently, the method calculates Power and Prioritized Coefficients, along with Generalized Power Prioritized Weighting Coefficient Factors. These coefficients and factors are then amalgamated into generalized power prioritized weighting coefficients, which are employed to consolidate Cq-RPFNs. To consolidate Cq-RPFNs, the MCDM utilizes the proposed AOs, Cq-RPFGPPYWA, and Cq-RPFGPPYWG. The final stage entails determining the score value for the amalgamated information to ascertain the ranking of alternatives. The decision-making process for the MCDM method is illustrated in Figure 7.

Step 1: Identifying Alternatives and Criteria: Let's examine a collection of alternatives, denoted as $\mathscr{E}_1, \mathscr{E}_2, \ldots, \mathscr{E}_n$, and a set of criteria represented by $\tau_1, \tau_2, \ldots, \tau_m$.

Step 2: Allocation of weights to individual criteria: Let ρ_i denote the weight assigned to criterion τ_i, where $\rho_i > 0$ for $i = 1, 2, \ldots, m$, and $\sum_{i=1}^{m} \rho_i = 1$.

Step 3: Evaluating Criteria against Alternatives with Cq-RPFNs: Each criterion τ_i $(i = 1, 2, \ldots, m)$ is evaluated against every alternative $\mathscr{Y}_j$ $(j = 1, 2, \ldots, n)$ using Cq-RPFNs. This evaluation is denoted as $\mathscr{Y}_{ij} = \langle(\mu_{ij}, \alpha_{ij}), (\nu_{ij}, \beta_{ij}), (\xi_{ij}, \gamma_{ij})\rangle$ for $i = 1, 2, \ldots, m$ and $j = 1, 2, \ldots, n$.

Step 4: Determine the Power Weighting Coefficients: The power weighting coefficients $\mathscr{S}_{ij}$ (Equation (2.8)) for each Cq-RPFN $\mathscr{Y}_{ij}$, where $i = 1, 2, \ldots, m$ and $j = 1, 2, \ldots, n$, are determined as follows.

$$\mathscr{S}_{ij} = \sum_{\substack{k=1 \\ k\neq i}}^{m} [1 - \mathscr{D}(\mathscr{Y}_{ij}, \mathscr{Y}_{kj})] \tag{2.31}$$

Here, the distance measure between $\mathscr{Y}_{ij}$ and $\mathscr{Y}_{kj}$ is determined using the following computation.

$$\mathscr{D}(\mathscr{Y}_{ij}, \mathscr{Y}_{kj}) = \frac{1}{6}\left(|\mu_{ij}^q - \mu_{kj}^q| + |\alpha_{ij}^q - \alpha_{kj}^q| + |\nu_{ij}^q - \nu_{kj}^q| + |\beta_{ij}^q - \beta_{kj}^q| + |\xi_{ij}^q - \xi_{kj}^q| + |\gamma_{ij}^q - \gamma_{kj}^q|\right)$$

Step 5: Determine the Prioritized Weighting Coefficients: The prioritized weighting coefficients $\mathscr{T}_{1j}$ (Equation (2.9)) and $\mathscr{T}_{ij}$ (Equation (2.10)) are computed for each Cq-RPFN $\mathscr{Y}_{ij}$, where $i = 1, 2, \ldots, m$ and $j = 2, \ldots, n$.

$$\mathscr{T}_{1j} = 1, \tag{2.32}$$

$$\mathscr{T}_{ij} = \prod_{k=1}^{i-1} \mathcal{S}(\mathscr{Y}_{kj}) \tag{2.33}$$

Here, the score function of $\mathscr{Y}_{kj}$ is determined using the following computation.

$$\mathcal{S}(\mathscr{Y}_{kj}) = \frac{1}{2} + \frac{1}{6}(\mu_{kj}^q + \alpha_{kj}^q - \nu_{kj}^q - \beta_{kj}^q - \xi_{kj}^q - \gamma_{kj}^q)$$

Step 6: Calculate the Generalized Power Prioritized Weighting Coefficient Factors: Express the generalized power prioritized weighting coefficient factors $\psi(i,j)$ by incorporating the criteria weights ρ_i (where i ranges from 1 to m), along with the parameters u and v constrained to the interval $[0, 1]$. This formulation involves the power weighting coefficients $\mathscr{S}_{ij}$ and the prioritized weighting coefficients $\mathscr{T}_{ij}$.

$$\psi(i,j) = \rho_i\,[u(1 + \mathscr{S}_{ij}) + v\mathscr{T}_{ij}] \tag{2.34}$$

Step 7: Find the Generalized Power Prioritized Weighting Coefficients: The generalized power prioritized weighting coefficients Θ_{ij} (Equation (2.11)) using Equation (2.34) are computed for each Cq-RPFN $\mathscr{Y}_{ij}$, where $i = 1, 2, \ldots, m$ and $j = 1, 2, \ldots, n$.

$$\Theta_{ij} = \frac{\psi(i,j)}{\sum_{k=1}^{m}\psi(i,j)} \tag{2.35}$$

Step 8: Aggregate Fuzzy Numbers: Combine all Cq-RPFN values $\mathscr{Y}_{1j}, \mathscr{Y}_{2j}, \ldots, \mathscr{Y}_{mj}$ $(j = 1, 2, \ldots, n)$ by employing either the AO, Cq-RPFGPPYWA (Equation 2.14), or Cq-RPFGPPYWG (Equation 2.29).

$$\text{Cq-RPFGPPYWA}(\mathscr{Y}_{1j}, \mathscr{Y}_{2j}, \ldots, \mathscr{Y}_{mj}) = \oplus_{i=1}^{m}\Theta_{ij}\mathscr{Y}_{ij}$$

$$= \left\langle \begin{array}{c} \left(\left[1 - \min\{1, (\sum_{i=1}^{m}\Theta_{ij}(1-\mu_{ij}{}^{q})^{\lambda})^{1/\lambda}\}\right]^{1/q}, \left[1 - \min\{1, (\sum_{i=1}^{m}\Theta_{ij}(1-\alpha_{ij}{}^{q})^{\lambda})^{1/\lambda}\}\right]^{1/q}\right), \\ \left(\left[\min\{1, (\sum_{i=1}^{m}\Theta_{ij}\nu_{ij}^{q\,\lambda})^{1/\lambda}\}\right]^{1/q}, \left[\min\{1, (\sum_{i=1}^{m}\Theta_{ij}\beta_{ij}^{q\,\lambda})^{1/\lambda}\}\right]^{1/q}\right), \\ \left(\left[\min\{1, (\sum_{i=1}^{m}\Theta_{ij}\xi_{ij}^{q\,\lambda})^{1/\lambda}\}\right]^{1/q}, \left[\min\{1, (\sum_{i=1}^{m}\Theta_{ij}\gamma_{ij}^{q\,\lambda})^{1/\lambda}\}\right]^{1/q}\right) \end{array} \right\rangle \tag{2.36}$$

(or)

$$\text{Cq-RPFGPPYWG}(\mathscr{Y}_{1j}, \mathscr{Y}_{2j}, \ldots, \mathscr{Y}_{mj}) = \otimes_{i=1}^{m}\Theta_{ij}\mathscr{Y}_{ij}$$

$$= \left\langle \begin{array}{c} \left(\left[\min\{1, (\sum_{i=1}^{m}\Theta_{ij}\mu_{ij}^{q\,\lambda})^{1/\lambda}\}\right]^{1/q}, \left[\min\{1, (\sum_{i=1}^{m}\Theta_{ij}\alpha_{ij}^{q\,\lambda})^{1/\lambda}\}\right]^{1/q}\right), \\ \left(\left[1 - \min\{1, (\sum_{i=1}^{m}\Theta_{ij}(1-\nu_{ij}{}^{q})^{\lambda})^{1/\lambda}\}\right]^{1/q}, \left[1 - \min\{1, (\sum_{i=1}^{m}\Theta_{ij}(1-\beta_{ij}{}^{q})^{\lambda})^{1/\lambda}\}\right]^{1/q}\right), \\ \left(\left[1 - \min\{1, (\sum_{i=1}^{m}\Theta_{ij}(1-\xi_{ij}{}^{q})^{\lambda})^{1/\lambda}\}\right]^{1/q}, \left[1 - \min\{1, (\sum_{i=1}^{m}\Theta_{ij}(1-\gamma_{ij}{}^{q})^{\lambda})^{1/\lambda}\}\right]^{1/q}\right) \end{array} \right\rangle \tag{2.37}$$

Step 9: **Calculate the Score Value:** The score value for the aggregated information in **Step 8** (Equation (2.36) or Equation (2.37)) is calculated by utilizing Equation (2.1).

Step 10: **Obtain the Rank of Alternatives:** The ranking of alternatives $\mathscr{E}_j$ $(j = 1, 2, \ldots, n)$ is obtained based on the score value calculated in **Step 9**.

mcdm (1).jpg

Fig. 7. Flowchart illustrating the decision-making process of the proposed MCDM method

3. Results

3.1 *Case Study*

This section delves into innovative approaches to power and energy in India, highlighting key initiatives such as Solar Energy, Wind Energy, Hydroelectric Power, and Biomass Energy.

3.1.1 *Solar Energy:*

India's solar energy sector has experienced significant growth, reaching an installed capacity of 97.86 GW by December 2024 [57]. With over 300 sunny days annually, India is ideal for solar power generation [58]. States like Rajasthan, Gujarat, and Tamil Nadu have set up large-scale solar parks, with Bhadla Solar Park in Rajasthan being one of the world's largest, with a capacity of 2,255 MW [58]. The government's efforts are further highlighted by the creation of the International Solar Alliance (ISA), aiming to promote solar energy globally [57]. However, challenges like land acquisition and grid integration remain key hurdles in sustaining this growth [58]. Further technological and policy innovation is needed to overcome these issues [57]. Addressing these challenges will be crucial for continuing India's solar energy progress [58].

3.1.2 *Wind Energy:*

India's wind energy capacity reached 48.16 GW by 2024, positioning the country as one of the top global leaders in wind energy [57]. With plans to reach 60 GW by 2030, India's wind energy sector holds significant untapped potential [59]. Combining wind and solar power offers a unique opportunity to address intermittency, as solar power peaks during the day and wind energy during the night [59]. The Indian government is investing in energy storage and grid modernization to address these challenges [57]. However, land acquisition for wind farms and infrastructure remains a bottleneck [59]. Efficient integration of wind power into the national grid is a critical next step for India's renewable energy growth [59]. Moreover, ongoing policy support and investment in storage solutions will be needed to overcome these barriers [57].

3.1.3 *Hydroelectric Power:*

India's hydroelectric potential exceeds 148 GW, with 46 GW still untapped, mostly in the Himalayan and northeastern regions [60]. Small hydropower plants, under 25 MW, present a significant opportunity for sustainable energy generation [57]. These plants contribute to the renewable energy mix by utilizing river streams for power production [60]. However, large-scale hydroelectric projects face environmental concerns and displacement issues [60]. The government is encouraging small and micro hydropower projects through policy incentives [57]. Yet, further investment and planning are needed for hydroelectric energy to reach its full potential [60]. Effective regulation and stakeholder engagement are crucial for balancing development with environmental preservation [60].

3.1.4 *Biomass Energy:*

Biomass energy in India contributes 10.72 GW, with the majority coming from bagasse-based cogeneration [61]. Biomass provides an opportunity for renewable energy, utilizing agricultural residues and organic waste materials [61]. This not only generates electricity but also helps manage agricultural waste, reducing the need for open burning and mitigating air pollution [61]. The government has provided incentives to promote biomass energy projects, and new technologies have made these plants more energy-efficient [57]. However, challenges such as feedstock availability and competition with other biomass uses remain [61]. Addressing these challenges requires further development of efficient biomass collection systems and clearer policies [61]. In the future, biomass energy could play a significant role in India's renewable energy strategy [57].

India's renewable energy sector has made significant strides, with ambitious goals to achieve 500 GW of renewable energy capacity by 2030 [62]. However, challenges such as land acquisition, environmental concerns, and waste disposal from renewable technologies continue to hinder progress [62]. Resolving these issues requires a balanced approach, integrating environmental, social, and economic considerations [62]. Additionally, developing proper waste recycling strategies for solar panels and EV batteries will be essential for sustainable growth in the renewable sector [63]. Managing the environmental impact of renewable energy technologies remains a key challenge moving forward [63]. Nonetheless, India's renewable energy experience offers valuable lessons for other developing nations transitioning toward a sustainable energy future [62].

This section presents the numerical results derived from the application of the proposed MCDM approach to assess and rank power and energy strategies in India. It includes sensitivity and comparative analyses of the identified alternatives, followed by a discussion on their implications and possible limitations.

3.2 Application of MCDM

In this subsection, we apply the MCDM methodology described in the Section to evaluate and rank energy and power strategies for India. To illustrate the effectiveness of the approach, we focus on four key strategies highlighted in the Case Study (Section 3.1), aligning with the primary goal of this paper to demonstrate the applicability of the MCDM framework in energy planning.

Step 1: Identifying Alternatives and Criteria: The options labeled as $\mathscr{E}_1$, $\mathscr{E}_2$, $\mathscr{E}_3$, and $\mathscr{E}_4$ correspond to Solar Energy, Wind Energy, Hydroelectric Power, and Biomass Energy respectively. The criteria τ_1, τ_2, τ_3, and τ_4 (Refer Table 1) serve as assessment parameters for energy solutions, specifically addressing resource availability, environmental impact, cost-effectiveness, and energy efficiency, respectively.

Table 1
Description and Significance of Key Evaluation Criteria for Renewable Energy Resources

Criteria	**Description**	**Importance**
Resource Availability [64]	Assessing the availability and abundance of the energy resource is essential to determine its long-term sustainability and reliability.	Ensures the long-term sustainability and reliability of energy solutions.
Environmental Impact [65]	Evaluating the environmental impact involves considering factors such as carbon emissions, land use, water consumption, and potential ecosystem disruption.	Helps select environmentally sustainable solutions, minimizing harm to ecosystems and public health.
Cost-effectiveness [66]	Analyzing the cost-effectiveness includes assessing factors such as initial investment costs, operational expenses, and the potential for economic returns or cost savings.	Impacts the economic viability of energy solutions, ensuring optimal resource allocation.
Energy Efficiency [67]	Evaluating energy efficiency involves assessing the conversion efficiency of the energy resource and its ability to maximize energy output relative to input.	Affects the overall performance and sustainability of energy solutions, although to a slightly lesser extent compared to other criteria.

Step 2: Allocation of weights to individual criteria for identification: Assume that $\rho_1 = 0.3$, $\rho_2 = 0.4$, $\rho_3 = 0.1$, and $\rho_4 = 0.2$ denote the weights assigned to criteria ρ_1, ρ_2, ρ_3, and ρ_4, respectively. It's essential to clarify that these weights are hypothetical and solely utilized for illustrative purposes within the framework of the proposed MCDM method (see Section 2.3).

Step 3: Evaluating Criteria Alternatives with Cq-RPFNs: Each criterion ρ_i $(i = 1, 2, \ldots, 4)$ is evaluated against each alternative $\mathscr{E}_j$ $(j = 1, 2, \ldots, 4)$ using the Cq-RPFN representation with $q = 5$, denoted as $\rho_{ij} = \langle(\mu_{ij}, \alpha_{ij}), (\nu_{ij}, \beta_{ij}), (\xi_{ij}, \gamma_{ij})\rangle$ for $i = 1, 2, \ldots, 4$ and $j = 1, 2, \ldots, 4$. The tabular representation of Cq-RPFN is provided in Table 2. It's crucial to highlight that the values illustrated in Table 2 are hypothetical and are employed for explanatory purposes within the framework of the proposed MCDM method (see Section 2.3).

Table 2
Tabular Representation of Cq-RPFNs ($q = 5$)

$(\tau/\mathscr{E})$	$\mathscr{E}_1$	$\mathscr{E}_2$	$\mathscr{E}_3$	$\mathscr{E}_4$
τ_1	$\langle(0.7, 0.3), (0.3, 0.2), (0.4, 0.2)\rangle$	$\langle(0.7, 0.6), (0, 0.3), (0.2, 0.1)\rangle$	$\langle(0.3, 0.4), (0.5, 0.4), (0.4, 0.5)\rangle$	$\langle(0.5, 0.4), (0.6, 0.7), (0.6, 0.2)\rangle$
τ_2	$\langle(0.5, 0.2), (0.2, 0.1), (0.4, 0.2)\rangle$	$\langle(0.4, 0.2), (0.1, 0.3), (0.2, 0)\rangle$	$\langle(0.1, 0.2), (0.4, 0.6), (0.5, 0.7)\rangle$	$\langle(0.3, 0.2), (0.2, 0.3), (0.5, 0.4)\rangle$
τ_3	$\langle(0.6, 0.4), (0.6, 0.5), (0.5, 0.1)\rangle$	$\langle(0.5, 0.4), (0.3, 0.5), (0.1, 0.2)\rangle$	$\langle(0.3, 0.4), (0.6, 0.7), (0.4, 0.5)\rangle$	$\langle(0.3, 0.3), (0.6, 0.5), (0, 0.2)\rangle$
τ_4	$\langle(0.5, 0.4), (0.3, 0.2), (0.4, 0.1)\rangle$	$\langle(0.6, 0.3), (0.4, 0.2), (0.3, 0.2)\rangle$	$\langle(0.4, 0.3), (0.5, 0.6), (0.6, 0.8)\rangle$	$\langle(0.7, 0.4), (0.5, 0.3), (0.2, 0.3)\rangle$

Step 4: Determine the Power Weighting Coefficients: The power weighting coefficients, denoted as $\mathscr{S}_{ij}$, are calculated for each Cq-RPFN $\mathscr{Y}_{ij}$ (Table 2), where $(i = 1, 2, \ldots 4,)$ and $(j = 1, 2, \ldots, 4)$. Specifically, we focus on the calculation of $\mathscr{S}_{11}$, and the remaining coefficients can be determined in a similar fashion. Referring to Equation 2.31, we obtain:

$$\mathscr{S}_{11} = [1 - \mathscr{D}(\mathscr{Y}_{11}, \mathscr{Y}_{21})] + [1 - \mathscr{D}(\mathscr{Y}_{11}, \mathscr{Y}_{31})] + [1 - \mathscr{D}(\mathscr{Y}_{11}, \mathscr{Y}_{41})] \tag{3.1}$$

In this scenario, the computation of the distance between $\mathscr{Y}_{11}$ and $\mathscr{Y}_{i1}$ $(i = 1, 2, 3, 4)$ as follows.

$$\mathscr{D}(\mathscr{Y}_{11}, \mathscr{Y}_{21}) = \frac{1}{6}\left(|\mu_{11}^q - \mu_{21}^q| + |\alpha_{11}^q - \alpha_{21}^q| + |\nu_{11}^q - \nu_{21}^q| + |\beta_{11}^q - \beta_{21}^q| + |\xi_{11}^q - \xi_{21}^q| + |\gamma_{11}^q - \gamma_{21}^q|\right) \tag{3.2}$$

Substituting the values of μ_{i1}, α_{i1}, ν_{i1}, β_{i1}, ξ_{i1}, and γ_{i1} (where $i = 1, 2$) from Table 2, along with $q = 5$, into Equation (3.2), yields $\mathscr{D}(\mathscr{Y}_{11}, \mathscr{Y}_{21}) = 0.0235583$. Similarly, calculating the distances results in $\mathscr{D}(\mathscr{Y}_{11}, \mathscr{Y}_{31}) = 0.0376167$, and, $\mathscr{D}(\mathscr{Y}_{11}, \mathscr{Y}_{41}) = 0.0241567$. By substituting these values into Equation (3.1), we find $\mathscr{S}_{11} = 2.9146683$. Similarly, the values for $\mathscr{S}_{ij}$ can be computed for $(i = 2, \ldots, 4)$ and $(j = 2, \ldots, 4)$ using the same methodology. The resulting power weighting coefficients $\mathscr{S}_{ij}$ for each Cq-RPFN $\mathscr{Y}_{ij}$ are summarized in Table 3.

Table 3
Power Weighting Coefficients $\mathscr{S}_{ij}$ for Table 2

$(\tau/\mathscr{E})$	$\mathscr{E}_1$	$\mathscr{E}_2$	$\mathscr{E}_3$	$\mathscr{E}_4$
τ_1	2.9146683	2.8913483	2.8483117	2.8303367
τ_2	2.9432617	2.9362517	2.862305	2.87783
τ_3	2.9023483	2.9342517	2.8252117	2.89134
τ_4	2.9447717	2.9399517	2.7995083	2.84584

Step 5: Compute the Prioritized Weighting Coefficients: The prioritized weighting coefficients, denoted as $\mathscr{T}_{ij}$, are computed for each Cq-RPFN $\mathscr{Y}_{ij}$ (Table 2), where $i = 1, 2, \ldots, 4$ and $j = 1, 2, \ldots, 4$. Specifically, we focus on the computation of $\mathscr{T}_{11}$, $\mathscr{T}_{21}$, $\mathscr{T}_{31}$, and the remaining coefficients can be determined similarly. From the equation labeled as Equation 2.32, we obtain

$$\mathscr{V}_{11} = 1$$

By referring to Equation 2.33, it follows that

$$\mathscr{T}_{21} = \mathcal{S}(\mathscr{Y}_{11}) = \frac{1}{2} + \frac{1}{6}(\mu_{11}^q + \alpha_{11}^q - \nu_{11}^q - \beta_{11}^q - \xi_{11}^q - \gamma_{11}^q) \tag{3.3}$$

$$\mathscr{T}_{31} = \mathcal{S}(\mathscr{Y}_{11})\mathcal{S}(\mathscr{Y}_{21}) = (\frac{1}{2}+\frac{1}{6}(\mu_{11}^{q}+\alpha_{11}^{q}-\nu_{11}^{q}-\beta_{11}^{q}-\xi_{11}^{q}-\gamma_{11}^{q}))(\frac{1}{2}+\frac{1}{6}(\mu_{21}^{q}+\alpha_{21}^{q}-\nu_{21}^{q}-\beta_{21}^{q}-\xi_{21}^{q}-\gamma_{21}^{q})) \tag{3.4}$$

Substituting the values of μ_{i1}, α_{i1}, ν_{i1}, β_{i1}, ξ_{i1} and γ_{i1} where $i = 1, 2$ from Table 2, alongside $q = 5$, into Equation (3.3) and Equation (3.4), we obtain $\mathscr{T}_{21} = 0.526198$ and $\mathscr{T}_{31} = 0.284416$. Similarly, the remaining values of $\mathscr{T}_{ij}$ can be computed by using the same methodology. The resulting prioritized weighting coefficients factors $\mathscr{T}_{ij}$ for each Cq-RPFN $\mathscr{Y}_{ij}$ are detailed in Table 4.

Table 4
Prioritized Weighting Coefficients $\mathscr{T}_{ij}$ for Table 2

$(\tau/\mathscr{E})$	$\mathscr{E}_1$	$\mathscr{E}_2$	$\mathscr{E}_3$	$\mathscr{E}_4$
τ_1	1	1	1	1
τ_2	0.5261983	0.5405117	0.4882817	0.45293
τ_3	0.2649128	0.2709585	0.2207855	0.223333
τ_4	0.1301486	0.135817	0.1002863	0.1077779

Step 6: Calculate the Generalized Power Prioritized Weighting Coefficient Factors: Assuming the parameters $u = 0.8$ and $v = 0.2$ in the interval $[0, 1]$, the generalized power prioritized weighting coefficient factors, denoted as ψ_{ij}, are computed for each Cq-RPFN $\mathscr{Y}_{ij}$ (Table 2), where $(i = 1, 2, \ldots, 4)$ and $(j = 1, 2, \ldots, 4)$. Specifically, we focus on the computation of ψ_{11}, and the remaining coefficients can be determined similarly. From referencing Equation 2.34, we derive:

$$\psi_{11} = \rho_1 [u(1 + \mathscr{S}_{11}) + v\mathscr{T}_{11}] \tag{3.5}$$

Replace ρ_1 with the weights of criteria obtained in **Step 2**, $\mathscr{S}_{11}$ with the corresponding value from Table 3, and $\mathscr{T}_{11}$ with the respective value from Table 4 in Equation 3.5. This yields $\psi_{11} = 0.8546403$. Similarly, for $(i = 2, \ldots, 4)$ and $(j = 2, \ldots, 4)$, ψ_{ij} values can be computed following the same procedure. The resulting generalized power prioritized weighting coefficient factors ψ_{ij} for each Cq-RPFN $\mathscr{Y}_{ij}$ are presented in detail in Table 5.

Table 5
The value of ψ_{ij} for the data in Table 3 and Table 4

$(\tau/\mathscr{E})$	$\mathscr{E}_1$	$\mathscr{E}_2$	$\mathscr{E}_3$	$\mathscr{E}_4$
τ_1	0.3237229	0.3222321	0.3274097	0.3256688
τ_2	0.3983363	0.3989061	0.3980879	0.3961999
τ_3	0.0937057	0.0945744	0.0934608	0.0949108
τ_4	0.1842351	0.1842874	0.1810415	0.1832205

Step 7: Find the Generalized Power Prioritized Weighting Coefficients: The generalized power prioritized weighting coefficients Θ_{ij}, are calculated individually for each Cq-RPFN $\mathscr{Y}_{ij}$ (Table 2), where $i = 1, 2, \ldots, 4$ and $j = 1, 2, \ldots, 4$. Specifically, our focus is on determining the value of Θ_{11}, with the remaining coefficients following a similar process. Referring to Equation (2.35),

we derive:

$$\Theta_{11} = \frac{\psi_{11}}{\sum_{i=1}^{4} \psi_{i1}} \tag{3.6}$$

Insert the value of ψ_{i1} $(i = 1, 2, \ldots, 4)$ from Table 5 into Equation (3.6). Upon calculation, Equation (3.6) produces $\Theta_{11} = 0.3237229$. Similarly, the values of Θ_{ij} can be computed for $i = 2, \ldots, 4$ and $j = 2, \ldots, 4$, following the same methodology. The resulting generalized power prioritized weighting coefficients Θ_{ij} for each Cq-RPFN $\mathscr{Y}_{ij}$ are detailed in Table 6.

Table 6
The value of Θ_{ij} for the data provided in Table 5

$(\tau/\mathscr{E})$	$\mathscr{E}_1$	$\mathscr{E}_2$	$\mathscr{E}_3$	$\mathscr{E}_4$
τ_1	0.8546403	0.8504427	0.8426961	0.8394606
τ_2	1.0516225	1.0528027	1.0246095	1.0212652
τ_3	0.2473865	0.249603	0.240552	0.244647
τ_4	0.4863875	0.4863759	0.4659696	0.4722786

Step 8: Aggregate Fuzzy Numbers: Aggregate each Cq-RPFN $\mathscr{Y}_{1j}, \mathscr{Y}_{2j}, \ldots, \mathscr{Y}_{4j}$ $(j = 1, 2, \ldots, 4)$ in Table 2 by using either the AO, Cq-RPFGPPYWA (Equation (2.36)) or Cq-RPFGPPYWG (Equation (2.37)). In particular, our attention is directed towards aggregating the Cq-RPFN $\mathscr{Y}_{11}, \mathscr{Y}_{21}, \ldots, \mathscr{Y}_{41}$ $(j = 1, 2, \ldots, 4)$ with respect to the AO, Cq-RPFGPPYWA $(q = 5)$, in the following manner.

$$\text{Cq-RPFGPPYWA}(\mathscr{Y}_{11}, \mathscr{Y}_{21}, \mathscr{Y}_{31}, \mathscr{Y}_{41}) = \oplus_{i=1}^{4} \Theta_{i1}\mathscr{Y}_{i1}$$

$$= \left\langle \begin{array}{c} \left(\left[1 - \min\{1, (\sum_{i=1}^{m} \Theta_{i1}(1-\mu_{i1}{}^{q})^{\lambda})^{1/\lambda}\}\right]^{1/q}, \left[1 - \min\{1, (\sum_{i=1}^{m} \Theta_{i1}(1-\alpha_{i1}{}^{q})^{\lambda})^{1/\lambda}\}\right]^{1/q}\right), \\ \left(\left[\min\{1, (\sum_{i=1}^{m} \Theta_{i1}\nu_{i1}^{q\lambda})^{1/\lambda}\}\right]^{1/q}, \left[\min\{1, (\sum_{i=1}^{m} \Theta_{i1}\beta_{i1}^{q\lambda})^{1/\lambda}\}\right]^{1/q}\right), \\ \left(\left[\min\{1, (\sum_{i=1}^{m} \Theta_{i1}\xi_{i1}^{q\lambda})^{1/\lambda}\}\right]^{1/q}, \left[\min\{1, (\sum_{i=1}^{m} \Theta_{i1}\gamma_{i1}^{q\lambda})^{1/\lambda}\}\right]^{1/q}\right) \end{array} \right\rangle \tag{3.7}$$

Substitute the values of Θ_{i1} $(i = 1, 2, \ldots, 4)$ from Table 6, and the values of μ_{i1}, α_{i1}, ν_{i1}, β_{i1}, ξ_{i1}, γ_{i1} $(i = 1, 2, \ldots, 4)$ from Table 2 into Equation (3.7). After computation, Equation (3.7) yields Cq-RPFGPPYWA$(\mathscr{Y}_{11}, \mathscr{Y}_{21}, \ldots, \mathscr{Y}_{41}) = \langle(0.5968, 0.3270), (0.5123, 0.4269), (0.4354, 0.1957)\rangle$. Similarly, aggregation of Cq-RPFNs, $\mathscr{Y}_{1j}, \mathscr{Y}_{2j}, \ldots, \mathscr{Y}_{4j}$ for $(j = 2, \ldots, 4)$ can be performed. Likewise, aggregation of Cq-RPFNs, $\mathscr{Y}_{1j}, \mathscr{Y}_{2j}, \ldots, \mathscr{Y}_{4j}$ $(j = 1, 2, \ldots, 4)$, as provided in Table 2, can be conducted using the AO, Cq-RPFGPPYWG (Equation (2.37)). The resulting aggregation values are displayed in Table 7.

Table 7
Aggregation values for Cq-RPFNs in Table 2 with respect to proposed operators

Alternative	**Cq-RPFGPPYWA Operator**
$\mathscr{E}_1$	$\langle(0.5968586, 0.3270764), (0.5123976, 0.4269935), (0.4354127, 0.195705)\rangle$
$\mathscr{E}_2$	$\langle(0.5884891, 0.4794238), (0.3575122, 0.4273581), (0.268171, 0.1836779)\rangle$
$\mathscr{E}_3$	$\langle(0.3100965, 0.3445454), (0.5229851, 0.6170809), (0.5403394, 0.7264006)\rangle$
$\mathscr{E}_4$	$\langle(0.5210838, 0.3538229), (0.5673901, 0.6496371), (0.5595902, 0.3762128)\rangle$
Alternative	**Cq-RPFGPPYWG Operator**
$\mathscr{E}_2$	$\langle(0.6510061, 0.3676534), (0.3822399, 0.3131903), (0.4140621, 0.1878348)\rangle$
$\mathscr{E}_3$	$\langle(0.651574, 0.556394), (0.2915224, 0.3422095), (0.232462, 0.1560164)\rangle$
$\mathscr{E}_4$	$\langle(0.357655, 0.37772), (0.4851063, 0.573261), (0.4967184, 0.6611549)\rangle$
$\mathscr{E}_1$	$\langle(0.6255934, 0.3824497), (0.5179436, 0.5559278), (0.5166194, 0.3410723)\rangle$

Step 9: Calculate the Score Value:

The score value for the aggregated information in Table 7 (**Step 8**) is calculated by utilizing Equation (2.1). The computed score values are displayed in Table 8.

Table 8
Score values for aggregated information provided in Table 7

Proposed Operator	$\mathscr{E}_1$	$\mathscr{E}_2$	$\mathscr{E}_3$	$\mathscr{E}_4$
Cq-RPFGPPYWA	0.5023395	0.5123697	0.438469	0.4678409
Cq-RPFGPPYWG	0.5166782	0.5271989	0.4613659	0.4953688

Step 10: Obtain the Rank of Alternatives: The ranking of alternatives $\mathscr{E}_j$ $(j = 1, 2, \ldots, n)$ is determined based on the score value calculated in Table 8 (**Step 9**). Table 9 presents the ranking of alternatives based on the proposed AOs, Cq-RPFGPPYWA and Cq-RPFGPPYWG $(q = 5)$.

Table 9
Ranking the Alternatives with respect to the Proposed AOs.

Proposed AOs	**Ranking**
Cq-RPFGPPYWA	$\mathscr{E}_2 \succ \mathscr{E}_1 \succ \mathscr{E}_4 \succ \mathscr{E}_3$
Cq-RPFGPPYWG	$\mathscr{E}_2 \succ \mathscr{E}_1 \succ \mathscr{E}_4 \succ \mathscr{E}_3$

3.3 *Exploring Sensitivity Analysis in Proposed Aggregation Operators*

This section includes two subsections: Subsection 3.3.1 presents a sensitivity analysis of the proposed AOs, Cq-RPFGPPYWA and Cq-RPFGPPYWG, across λ, u, and v, with q fixed. Subsection 3.3.2 analyzes the sensitivity across q, u, and v, while keeping λ fixed.

3.3.1 *Sensitivity Analysis Across Parameters λ, u, and v, with q fixed*

This section examines the sensitivity of the AOs Cq-RPFGPPYWA and Cq-RPFGPPYWG to variations in λ, u, and v, with q fixed at 5. As shown in Table 10, the ranking remains consistent despite changes in λ, u, and v, highlighting that lower values of q have minimal impact on the ranking. For $\lambda = 30, 90$, the scores increase with decreasing u and increasing v, while for $\lambda = 180, 200$, the scores fluctuate but the ranking is unaffected. This suggests that the ranking is stable across a range of λ and u, v values. Figure 8 visualizes the stability of alternative scores as λ varies, with q fixed at 5.

Table 10
Sensitivity analysis of proposed AOs across λ, u, and v, with q fixed at 5

q	u	v	λ	**Proposed Operator**	**Score Values**				**Ranking**
					$\mathscr{E}_1$	$\mathscr{E}_2$	$\mathscr{E}_3$	$\mathscr{E}_4$	
5	1	0	30	Cq-RPFGPPYWA	0.4866102	0.5009157	0.3992426	0.45025	$\mathscr{E}_2 \succ \mathscr{E}_1 \succ \mathscr{E}_4 \succ \mathscr{E}_3$
				Cq-RPFGPPYWG	0.525389	0.5382061	0.4781912	0.5169239	
	0.7	0.6	90	Cq-RPFGPPYWA	0.4838642	0.4971503	0.3948513	0.4473996	$\mathscr{E}_2 \succ \mathscr{E}_1 \succ \mathscr{E}_4 \succ \mathscr{E}_3$
				Cq-RPFGPPYWG	0.5268228	0.5395811	0.4867564	0.5232137	
	0.6	0.9	180	Cq-RPFGPPYWA	0.4830658	0.4980449	0.3935412	0.4480642	$\mathscr{E}_2 \succ \mathscr{E}_1 \succ \mathscr{E}_4 \succ \mathscr{E}_3$
				Cq-RPFGPPYWG	0.5255737	0.5400139	0.486386	0.5241349	
	0	1	200	Cq-RPFGPPYWA	0.4831936	0.498155	0.3941433	0.4481078	$\mathscr{E}_2 \succ \mathscr{E}_1 \succ \mathscr{E}_4 \succ \mathscr{E}_3$
				Cq-RPFGPPYWG	0.5257675	0.540294	0.4875491	0.5229972	

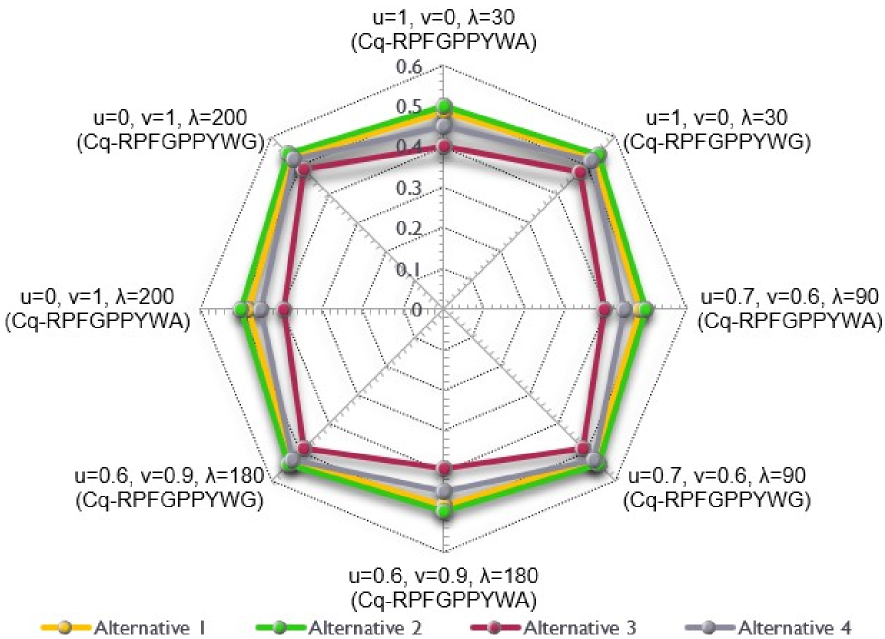

Fig. 8. Scores variation with changing u, v, and λ at fixed $q = 5$ for Cq-RPFGPPYWA and Cq-RPFGPPYWG operators

3.3.2 *Sensitivity Analysis Across Parameters* q, u, *and* v, *with* λ *Fixed*

This section analyzes the sensitivity of the AOs, Cq-RPFGPPYWA and Cq-RPFGPPYWG, across parameters q, u, and v, while fixing λ at 5. As shown in Table 11, the ranking remains stable despite variations in q, u, and v, especially at lower values of λ. The analysis indicates that changes in u (from 1 to 0.5) and v (from 0 to 0.8) do not affect the ranking for $q = 10, 15, 20$. However, when $q = 70$, $u = 0$, and $v = 1$, the scores for all alternatives become identical, suggesting that high values of q, such as $q = 70$, should be avoided. This finding allows decision-makers to select lower values of q while maintaining a consistent ranking with a fixed lower value of λ. Figure 9 visually demonstrates the stability of scores as q changes, with λ fixed at 5.

Table 11
Sensitivity analysis of proposed AOs across q, u, and v, with λ fixed at 5

λ	u	v	q	**Proposed Operator**	**Score Values** $\mathscr{E}_1$	$\mathscr{E}_2$	$\mathscr{E}_3$	$\mathscr{E}_4$	**Ranking**
5	1	0	10	Cq-RPFGPPYWA	0.5007234	0.5017702	0.4827104	0.495613	$\mathscr{E}_2 \succ \mathscr{E}_1 \succ \mathscr{E}_4 \succ \mathscr{E}_3$
				Cq-RPFGPPYWG	0.5035649	0.5044706	0.4934935	0.5012497	
	0.6	0.7	15	Cq-RPFGPPYWA	0.5002178	0.5003	0.4952511	0.4993775	$\mathscr{E}_2 \succ \mathscr{E}_1 \succ \mathscr{E}_4 \succ \mathscr{E}_3$
				Cq-RPFGPPYWG	0.5006272	0.5006978	0.4985504	0.5002352	
	0.5	0.8	20	Cq-RPFGPPYWA	0.5000424	0.5000488	0.4985585	0.4999054	$\mathscr{E}_2 \succ \mathscr{E}_1 \succ \mathscr{E}_4 \succ \mathscr{E}_3$
				Cq-RPFGPPYWG	0.5001069	0.5001124	0.4996059	0.500043	
	0	1	70	Cq-RPFGPPYWA	0.5	0.5	0.5	0.5	$\mathscr{E}_2 = \mathscr{E}_1 = \mathscr{E}_4 = \mathscr{E}_3$
				Cq-RPFGPPYWG	0.5	0.5	0.5	0.5	

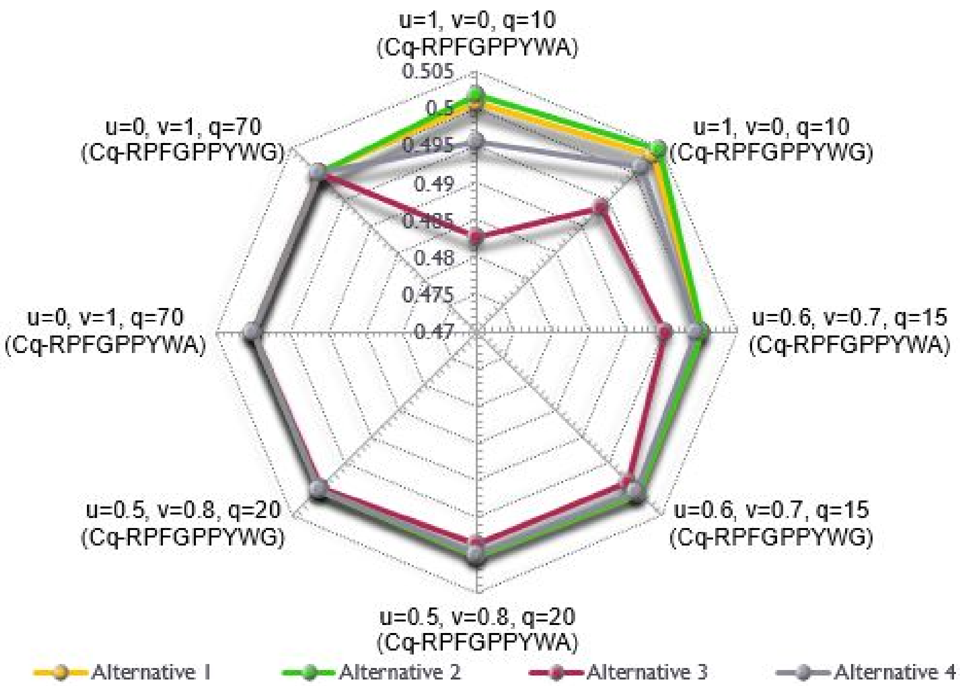

Fig. 9. Scores variation with changing u, v, and q at fixed $\lambda = 5$ for Cq-RPFGPPYWA and Cq-RPFGPPYWG operators

3.4 Comparative Analysis of Proposed Aggregation Operators with Existing Counterparts

In this section, we delve into two subsections: firstly, in subsection 3.4.1, we undertake a comparative examination of the proposed AOs, namely Cq-RPFGPPYWA and Cq-RPFGPPYWG, against the existing AOs within the Cq-RPFS framework. Additionally, in subsection 3.4.2, we conduct a comparative analysis of the proposed AOs, Cq-RPFGPPYWA and Cq-RPFGPPYWG, with the established AOs in Cq-ROFS, q-RPFS, PFS, and q-ROFS.

3.4.1 Comparison with Existing Aggregation Operators in Cq-RPFS Environments

Table 12 compares existing AOs in Cq-RPFS environments with the proposed AOs. In the "Descriptive Example," Cq-RPFEWA [33] ranks $\mathscr{E}_5$ above $\mathscr{E}_3$, followed by $\mathscr{E}_2$, $\mathscr{E}_4$, and $\mathscr{E}_1$. The proposed AOs, Cq-RPFGPPYWA and Cq-RPFGPPYWG, introduce new rankings favoring different entities, demonstrating their versatility. In "Table 8" [17], Cq-RPFFWA and Cq-RPFFWG rank $\mathscr{E}_4$ above $\mathscr{E}_5$, $\mathscr{E}_3$, $\mathscr{E}_1$, and $\mathscr{E}_2$, while the proposed AOs maintain this order, showing consistency. Similarly, in "Example 5.1" [18], Cq-RPFAAPOWA and Cq-RPFAAPOWG rank $\mathscr{E}_4$ above $\mathscr{E}_3$, $\mathscr{E}_5$, $\mathscr{E}_1$, and $\mathscr{E}_2$, with the proposed AOs preserving this ranking. This comparison highlights the robustness and adaptability of the proposed AOs across various scenarios, as shown in Figure 10.

Table 12
Comparison with Existing Aggregation Operators in Cq-RPFS Environments

Problem and Existing AOs	**Ranking**	**Proposed AOs** (q=4, λ=3, u=0.3, v=0.1)	**Ranking**
Example, Cq-RPFEWA [33]	$\mathscr{E}_5 \succ \mathscr{E}_3 \succ \mathscr{E}_2 \succ \mathscr{E}_4 \succ \mathscr{E}_1$	Cq-RPFGPPYWA,	$\mathscr{E}_5 \succ \mathscr{E}_2 \succ \mathscr{E}_4 \succ \mathscr{E}_1 \succ \mathscr{E}_3$
		Cq-RPFGPPYWG	$\mathscr{E}_5 \succ \mathscr{E}_2 \succ \mathscr{E}_4 \succ \mathscr{E}_3 \succ \mathscr{E}_1$
Table 8, Cq-RPFFWA, Cq-RPFFWG (q=10, $\lambda = 4$) [17]	$\mathscr{E}_4 \succ \mathscr{E}_5 \succ \mathscr{E}_3 \succ \mathscr{E}_1 \succ \mathscr{E}_2$	Cq-RPFGPPYWA, Cq-RPFGPPYWG	$\mathscr{E}_4 \succ \mathscr{E}_5 \succ \mathscr{E}_3 \succ \mathscr{E}_1 \succ \mathscr{E}_2$
Example 5.1, Cq-RPFAAPOWA, Cq-RPFAAPOWG [18]	$\mathscr{E}_5 \succ \mathscr{E}_1 \succ \mathscr{E}_2 \succ \mathscr{E}_4 \succ \mathscr{E}_3$	Cq-RPFGPPYWA, Cq-RPFGPPYWG	$\mathscr{E}_4 \succ \mathscr{E}_3 \succ \mathscr{E}_5 \succ \mathscr{E}_1 \succ \mathscr{E}_2$

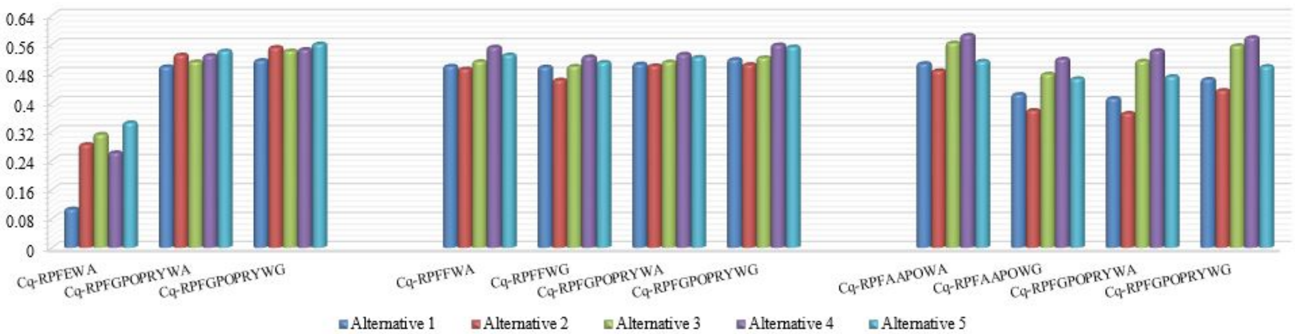

Fig. 10. Comparative Analysis of Existing and Proposed AOs in Cq-RPFS Environments

3.4.2 Comparison with Existing AOs in Cq-ROFS, q-RPFS, PFS, and q-ROFS Environments

Table 13 compares structure representations within the Cq-RPFN model, highlighting various structures, conditions, and representations. The Cq-ROFN structure is represented as a tuple with membership and non-membership functions under specific conditions. The q-RPFN structure introduces three parameters with similar conditions to Cq-ROFN, but with additional constraints. The PFN structure also includes three parameters but imposes stricter conditions on membership functions. The q-ROFN structure simplifies the representation by excluding the non-membership function parameter. This analysis clarifies the diverse representations in Cq-RPFN structures, aiding in the selection of the appropriate structure for specific fuzzy logic applications. It also compares existing aggregation operators in Cq-ROFS, q-RPFS, PFS, and q-ROFS with the proposed AOs in Cq-RPFN.

Table 13
Comparison of Structure Representations in the Cq-RPFN Model

Structure	Structure Representation	Condition	Cq-RPFN Representation
Cq-ROFN	$\langle(\mu_t, \alpha_t), (\xi_t, \gamma_t)\rangle$	$\mu_t^q + 0_t^q + \xi_t^q \leqslant 1, \alpha_t^q + 0_t^q + \gamma_t^q \leqslant 1\,(q \geqslant 1)$	$\langle(\mu_t, \alpha_t), (0, 0), (c_t, \gamma_t)\rangle$
q-RPFN	$\langle\mu_t, \nu_t, \xi_t\rangle$	$\mu_t^q + \nu_t^q + \xi_t^q \leqslant 1, 0_t^q + 0_t^q + 0_t^q \leqslant 1\,(q \geqslant 1)$	$\langle(\mu_t, 0), (\nu_t, 0), (\xi_t, 0)\rangle$
PFN	$\langle\mu_t, \nu_t, \xi_t\rangle$	$\mu_t^q + \nu_t^q + \xi_t^q \leqslant 1, 0_t^q + 0_t^q + 0_t^q \leqslant 1\,(q = 1)$	$\langle(\mu_t, 0), (\nu_t, 0), (\xi_t, 0)\rangle$
q-ROFN	$\langle\mu_t, \xi_t\rangle$	$\mu_t^q + 0_t^q + \xi_t^q \leqslant 1, 0_t^q + 0_t^q + 0_t^q \leqslant 1\,(q \geqslant 1)$	$\langle(\mu_t, 0), (0, 0), (\xi_t, 0)\rangle$

Table 14 compares existing AOs in Cq-ROFS, q-RPFS, PFS, and q-ROFS environments with the proposed ones, highlighting their performance through ranked assessments. In Example 3, Cq-ROPWDSM [68], the proposed Cq-RPFGPPYWA and Cq-RPFGPPYWG, with parameters $q = 4$, $\lambda = 3$, $u = 0.3$, and $\nu = 0.1$, consistently rank $\mathscr{E}_2 \succ \mathscr{E}_1 \succ \mathscr{E}_4 \succ \mathscr{E}_3$. In Example 1, Cq-ROFFWA [69], the proposed Cq-RPFGPPYWA maintains the ranking $\mathscr{E}_5 \succ \mathscr{E}_1 \succ \mathscr{E}_2 \succ \mathscr{E}_4 \succ \mathscr{E}_3$, while Cq-ROFFWG [69] ranks $\mathscr{E}_5 \succ \mathscr{E}_2 \succ \mathscr{E}_1 \succ \mathscr{E}_4 \succ \mathscr{E}_3$ with the same parameters. Table 1, focusing on q-RPFYWA [43], sets a reference ranking of $\mathscr{E}_1 \succ \mathscr{E}_2 \succ \mathscr{E}_4 \succ \mathscr{E}_3$, with the proposed AOs, Cq-RPFGPPYWA and Cq-RPFGPPYWG, confirming this order for parameters $q = 3$, $\lambda = 2$, $u = 1$, and $\nu = 1$. In Table 1, PFAAWA [70], the ranking $\mathscr{E}_5 \succ \mathscr{E}_2 \succ \mathscr{E}_4 \succ \mathscr{E}_1 \succ \mathscr{E}_3$ aligns with the proposed Cq-RPFGPPYWA, configured with $q = 1$, $\lambda = 2$, $u = 1$, and $\nu = 1$. Example 5.1, q-ROFDWA ($\kappa = 0.5$) [71], shows the proposed Cq-RPFGPPYWA ($q = 3$, $\lambda = 0.5$, $u = 0.1$, $\nu = 0.7$) aligns with the ranking $\mathscr{E}_1 \succ \mathscr{E}_4 \succ \mathscr{E}_3 \succ \mathscr{E}_2 \succ \mathscr{E}_5$. Lastly, Table 3, covering q-ROFWNA and q-ROFHNA [72], demonstrates that Cq-RPFGPPYWA and Cq-RPFGPPYWG, both with $q = 9$, $\lambda = 1$, $u = 1$, and $\nu = 1$, align with the ranking $\mathscr{E}_5 \succ \mathscr{E}_2 \succ \mathscr{E}_3 \succ \mathscr{E}_4 \succ \mathscr{E}_1$. This comparison highlights the versatility and effectiveness of the proposed AOs in various decision-making contexts, as shown in Figure 11.

Table 14
Comparison with Existing AOs in Cq-ROFS, q-RPFS, PFS, and q-ROFS Environments

Problem and Existing AOs	Ranking	Proposed AOs	Ranking
Example 3, Cq-ROPWDSM [68]	$\mathscr{E}_2 \succ \mathscr{E}_1 \succ \mathscr{E}_4 \succ \mathscr{E}_3$	Cq-RPFGPPYWA, Cq-RPFGPPYWG (q=4, λ=3, u=0.3, v=0.1)	$\mathscr{E}_2 \succ \mathscr{E}_1 \succ \mathscr{E}_4 \succ \mathscr{E}_3$
Example 1, Cq-ROFFWA [69]	$\mathscr{E}_5 \succ \mathscr{E}_2 \succ \mathscr{E}_1 \succ \mathscr{E}_4 \succ \mathscr{E}_3$	Cq-RPFGPPYWA (q=1.5, λ=3, u=0.3, v=0.1)	$\mathscr{E}_5 \succ \mathscr{E}_1 \succ \mathscr{E}_2 \succ \mathscr{E}_4 \succ \mathscr{E}_3$
Example 1, Cq-ROFFWG [69]	$\mathscr{E}_5 \succ \mathscr{E}_1 \succ \mathscr{E}_2 \succ \mathscr{E}_4 \succ \mathscr{E}_3$	Cq-RPFGPPYWG (q=1.5, λ=3, u=0.3, v=0.1)	$\mathscr{E}_5 \succ \mathscr{E}_2 \succ \mathscr{E}_1 \succ \mathscr{E}_4 \succ \mathscr{E}_3$
Table 1, q-RPFYWA, $(\upsilon = 1)$ [43]	$\mathscr{E}_1 \succ \mathscr{E}_2 \succ \mathscr{E}_4 \succ \mathscr{E}_3$	Cq-RPFGPPYWA, Cq-RPFGPPYWG (q=3, λ=2, u=1, v=1)	$\mathscr{E}_1 \succ \mathscr{E}_2 \succ \mathscr{E}_4 \succ \mathscr{E}_3$
Table 1, PFAAWA [70]	$\mathscr{E}_5 \succ \mathscr{E}_2 \succ \mathscr{E}_4 \succ \mathscr{E}_1 \succ \mathscr{E}_3$	Cq-RPFGPPYWA (q=1, λ=2, u=1, v=1)	$\mathscr{E}_5 \succ \mathscr{E}_1 \succ \mathscr{E}_4 \succ \mathscr{E}_2 \succ \mathscr{E}_3$
Example 5.1, q-ROFDWA $(\kappa = 0.5)$ [71]	$\mathscr{E}_1 \succ \mathscr{E}_4 \succ \mathscr{E}_3 \succ \mathscr{E}_2 \succ \mathscr{E}_5$	Cq-RPFGPPYWA (q=3, λ=0.5, u=0.1, v=0.7)	$\mathscr{E}_1 \succ \mathscr{E}_4 \succ \mathscr{E}_3 \succ \mathscr{E}_2 \succ \mathscr{E}_5$
Table 3, q-ROFWNA, q-ROFHNA [72]	$\mathscr{E}_5 \succ \mathscr{E}_3 \succ \mathscr{E}_2 \succ \mathscr{E}_4 \succ \mathscr{E}_1$	Cq-RPFGPPYWA, Cq-RPFGPPYWG (q=4, λ=3, u=1, v=1)	$\mathscr{E}_5 \succ \mathscr{E}_3 \succ \mathscr{E}_2 \succ \mathscr{E}_4 \succ \mathscr{E}_1$

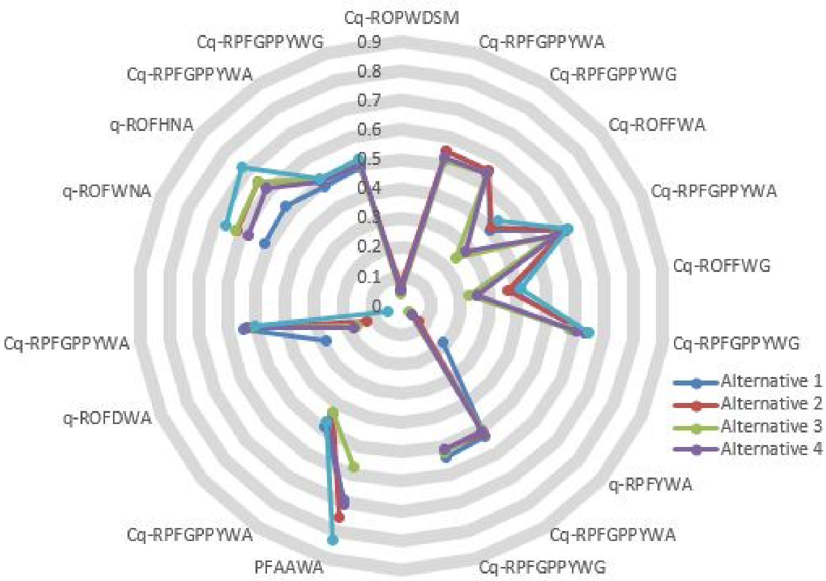

Fig. 11. Comparative Analysis of Existing and Proposed AOs in Cq-ROFS, q-RPFS, PFS, and q-ROFS

4. Conclusion

This study introduces novel operations and aggregation techniques within Cq-RPFNs, expanding fuzzy set theory with Yeager's operations, including addition, multiplication, scalar product, and scalar power operations. We developed two AOs—the Cq-RPFGPPYWA and the Cq-RPFGPPYWG—designed for aggregating fuzzy data in complex decision-making scenarios. Through the exploration of key properties like idempotency, monotonicity, and boundedness, we confirmed their robustness. Additionally, the proposed MCDM method, demonstrated through a case study in India's Power and Energy Sector, provides a systematic approach for handling uncertainty. Our comparative analysis with existing methods highlights the superiority of our approach, which offers significant practical value in addressing complex decision-making challenges across various domains.

4.1 Implementation of the Proposed Study

The implementation of the proposed study involves translating the theoretical methodologies into practical applications. Key steps include developing software or algorithms to integrate the introduced operations, aggregation operators, and decision-making methods, using programming languages like Python, MATLAB, or R. Real-world data will be represented through Cq-RPFNs where applicable, with algorithms incorporated into existing systems or decision support tools. Thorough testing and validation using both synthetic and real-world datasets will ensure the accuracy and robustness of the methods. The implemented techniques will then be applied to real-world case studies, such as India's Power and Energy Sector in 2024, and compared with existing approaches. Documentation of the implementation process, including software details, datasets, and results, will be disseminated through research papers and presentations. Feedback from stakeholders and practitioners will be gathered to refine and improve the methods iteratively, ensuring they address real-world challenges effectively.

4.2 Limitations of the Proposed Study

While the study provides valuable insights, there are several limitations. First, the scope of the study may limit its generalizability, as it focuses on specific aspects of complex q-rung picture fuzzy sets or certain application domains. Assumptions and simplifications may have oversimplified real-world complexities. The effectiveness of the proposed methodologies depends on the availability and quality of data, which could be limited. The introduced algorithms may also pose challenges in terms of computational complexity and resource requirements. The evaluation metrics used might not capture all relevant decision-making aspects, and effective application may require specialized expertise, which could hinder adoption. Additionally, the findings may have limited external validity, as they are based on specific contexts or datasets. The study may lack comprehensive comparisons with alternative methods, affecting understanding of relative advantages. Future uncertainties and ethical considerations may not have been fully addressed, potentially impacting the relevance and societal implications of the proposed techniques.

4.3 Future Research Directions

Future research can expand on the current study in several ways. First, extending Yager's operations to other fuzzy numbers and sets, and evaluating their applications in various fields, would showcase their versatility. Refining aggregation operators to handle more criteria, improve efficiency, and integrate frameworks like hesitant or interval-valued fuzzy sets could further enhance their utility. Additionally, expanding the proposed multi-criteria decision-making approach to dynamic environments, real-time data, and uncertainty handling, along with machine learning integration, would improve decision-making accuracy. Broader case studies across sectors such as healthcare, finance, and environmental management will strengthen the global applicability of these methods. Developing user-friendly software tools will ease adoption, while interdisciplinary collaborations can provide fresh insights, fostering innovative applications and improving the practical impact of the proposed methods.

Appendix

Table 15

Abbreviations

Abbreviation	**Full Form**
AO	Aggregation Operator
CIFS	Complex Intuitionistic Fuzzy Sets
CFS	Complex Fuzzy Sets
CPFS	Complex Picture Fuzzy Sets
CPyFS	Complex Pythagorean Fuzzy Set
Cq-RPFNs	Complex q-rung Picture Fuzzy Numbers
Cq-RoFS	Complex q-rung ortho-pair fuzzy set
Cq-RPFGPPYWA	Complex q-rung Picture Fuzzy Generalized Power Prioritized Yager Weighted Average
Cq-RPFGPPYWG	Complex q-rung Picture Fuzzy Generalized Power Prioritized Yager Weighted Geometric
Cq-RPFPOYWA	Complex q-rung Picture Fuzzy Power Yager Weighted Average
Cq-RPFPOYWG	Complex q-rung Picture Fuzzy Power Yager Weighted Geometric
Cq-RPFPRYWA	Complex q-rung Picture Fuzzy Prioritized Yager Weighted Average
Cq-RPFPRYWG	Complex q-rung Picture Fuzzy Prioritized Yager Weighted Geometric
Cq-RPFS	Complex q-rung Picture Fuzzy Set
Cq-ROFFWA	Complex q-Rung Orthopair Fuzzy Frank Weighted Average
Cq-ROFFWG	Complex q-Rung Orthopair Fuzzy Frank Weighted Geometric
Cq-ROPWDSM	Complex q-Rung Orthopair Weighted Dice Similarity Measures
Cq-RPFAAPOWA	Complex q-rung Picture Fuzzy Aczel–Alsina Prioritized Ordered Weighted Average
Cq-RPFAAPOWG	Complex q-rung Picture Fuzzy Aczel–Alsina Prioritized Ordered Weighted Geometric
Cq-RPFEWA	Complex q-Rung Picture Fuzzy Einstein Weighted Average
Cq-RPFFWG	Complex q-rung Picture Fuzzy Frank Weighted Geometric
Cq-RPFFWA	Complex q-rung Picture Fuzzy Frank Weighted Average
FS	Fuzzy Set
IFS	Intuitionistic Fuzzy Sets
MCDM	Multi-Criteria Decision-Making
NAPCC	National Action Plan on Climate Change
PFAAWA	Picture Fuzzy Aczel-Alsina Weighted Average
PFS	Picture Fuzzy Sets
POA	Power Average
PRA	Prioritized Average
PyFS	Pythagorean Fuzzy Sets
PyPFS	Pythagorean Picture Fuzzy Sets
q-ROFDWA	q-Rung Orthopair Fuzzy Dombi Weighted Average
q-ROFWNA	q-Rung Orthopair Fuzzy Weighted Neutral Average
q-ROFHNA	q-Rung Orthopair Fuzzy Hybrid Neutral Average
q-RPFYWA	q-Rung Picture Fuzzy Yager Weighted Average
q-ROFS	q-Rung Ortho-pair Fuzzy Set
q-RPFS	q-Rung Picture Fuzzy Sets
YTCN	Yager’s t-conorm
YTN	Yager’s t-norm

Acknowledgement

Not Applicable

Conflicts of Interest

The authors declare no conflicts of interest.

References

[1] Bharatee, A., Ray, P., Subudhi, B., & Ghosh, A. (2022). Power management strategies in a hybrid energy storage system integrated ac/dc microgrid: A review. *Energies*, *15*(19), 7176. https://doi.org/10.3390/en15197176
[2] Ghasemi, N., Ghanbari, M., & Ebrahimi, R. (2023). Intelligent and optimal energy management strategy to control the micro-grid voltage and frequency by considering the load dynamics and transient stability. *International Journal of Electrical Power and Energy Systems*, *145*, 108618. https://doi.org/10.1016/j.ijepes.2022.108618
[3] Bao, Y., Li, R., Yang, X., Saini, G., Krishna, P., & Wang, G. (2023). Optimal planning and multi-criteria decision-making for effective design and performance of hybrid microgrid integrated with energy management strategy. *Sustainable Energy Technologies and Assessments*, *56*, 103074. https://doi.org/10.1016/j.seta.2023.103074
[4] Karunathilake, E., Le, A., Heo, S., Chung, Y., & Mansoor, S. (2023). The path to smart farming: Innovations and opportunities in precision agriculture. *Agriculture*, *13*(8), 1593. https://doi.org/10.3390/agriculture13081593
[5] Liu, J., Ma, L., & Wang, Q. (2023). Energy management method of integrated energy system based on collaborative optimization of distributed flexible resources. *Energy*, *264*, 125981. https://doi.org/10.1016/j.energy.2022.125981
[6] Kandpal, V., Jaswal, A., Santibanez Gonzalez, E., & Agarwal, N. (2024). *Environmental impact assessment and sustainable energy transition*. Cham: Springer Nature Switzerland. https://doi.org/10.1007/978-3-031-52943-6_9
[7] Yu, S., You, L., & Zhou, S. (2023). A review of optimization modeling and solution methods in renewable energy systems. *Frontiers of Engineering Management*, *10*(4), 640–671. https://doi.org/10.1007/s42524-023-0271-3
[8] Chen, X., Chen, C., Tian, G., Yang, Y., Yong, X., & Zhao, Y. (2023). Comprehensive evaluation research of hybrid energy systems driven by renewable energy based on fuzzy multi-criteria decision-making. *Available at SSRN*, *4579594*. https://doi.org/10.3389/fenrg.2023.1294391
[9] Flickr. (n.d.). https://www.flickr.com/photos/192315865%40N02/50997746456/
[10] Led street light [[accessed Feb 6, 2024]]. (n.d.). https://cn.kompass.com/p/huaxia-led-video-display-screen-and-led-lighting/cn228934/led-street-light-led-wall-washer-light-led-pixel-light-strips/cd2c66f7-a1bd-4b0f-9211-6a8cfad71b79/
[11] Wave swell energy ltd [[accessed Feb 8, 2024]]. (n.d.). https://tethys.pnnl.gov/organization/wave-swell-energy-ltd
[12] Model, W. E. M. 3. (n.d.). Wave energy machine 3d model [[accessed Feb 8, 2024]]. https://free3d.com/3d-model/wave-energy-machine-9583.html
[13] grid: Integrating large-scale battery energy into the electricity network, P. (n.d.). Power grid: Integrating large-scale battery energy into the electricity network [[accessed Feb 8, 2024]]. https://roboticsandautomationnews.com/2018/07/17/power-grid-integrating-large-scale-battery-energy-into-the-electricity-network/18337/
[14] Tech, T. R. O. I. I. S. G. (n.d.). The role of iot in smart grid tech [[accessed Feb 9, 2024]]. https://www.intuz.com/blog/the-role-of-iot-in-smart-grid-tech

[15] Energy. (n.d.). 8 ways of generating electricity at home [[accessed Feb 9, 2024]]. https://diynewtech.com/8-ways-of-generating-electricity-at-home/
[16] Leadership, M. O. D. M.-T. I. C. (n.d.). Micro offsets driving macro-transformation in climate leadership [[accessed Feb 9, 2024]]. https://enkingint.org/micro-offsets-driving-macro-transformation-in-climate-leadership/
[17] M., F. B., Petchimuthu, S., Kamacı, H., & Senapati, T. (2024). Evaluation of artificial intelligence-based solid waste segregation technologies through multi-criteria decision-making and complex q-rung picture fuzzy frank aggregation operators. *Engineering Applications of Artificial Intelligence*, *133*, 108154. https://doi.org/10.1016/j.engappai.2024.108154
[18] Senapati, S. P. B. P. F. B. M. T. (2024). Exploring pharmacological therapies through complex q-rung picture fuzzy aczel–alsina prioritized ordered operators in adverse drug reaction analysis. *Engineering Applications of Artificial Intelligence*, *133*, 107996. https://doi.org/10.1016/j.engappai.2024.107996
[19] Subramanian Petchimuthua. Fathima Banu M. S. Thiruvazhimarba Pillaib, T. S. (n.d.). Advancing greenhouse gas emission reduction strategies: Integrating multi-criteria decision-making with complex q-rung picture fuzzy sugeno-weber operators [communicated].
[20] Pamucar, S. P. F. B. M. M. R. D. (n.d.). Water resource management optimization model for decision analytics using complex q-rung picture fuzzy information and yager power operators [communicated].
[21] Zadeh, L. A. (1965). Fuzzy sets. *Information and Control*, *8*(3), 338–353. https://doi.org/10.1007/978-1-4899-1633-4_2
[22] Atanassov, K. T. (1989). More on intuitionistic fuzzy sets. *Fuzzy sets and systems*, *33*(1), 37–45. https://doi.org/10.1016/0165-0114(89)90215-7
[23] Yager, R. (1994). Aggregation operators and fuzzy systems modeling. *Fuzzy Set Syst*, *67*(2), 129–145. https://doi.org/10.1016/0165-0114(94)90082-5
[24] Yager, R. R. (2016). Generalized orthopair fuzzy sets. *IEEE Transactions on Fuzzy Systems*, *25*(5), 1222–1230. https://doi.org/10.1109/TFUZZ.2016.2604005
[25] Cuong, B. C., & Kreinovich, V. (2013). Picture fuzzy sets new concepts for computational intelligence problems. *2013 Third World Congress on Information and Communication Technologies (WICT 2013)*, 1–6. https://doi.org/10.1109/WICT.2013.7113099
[26] Cuong, B. C. (2019). Pythagorean picture fuzzy sets, part 1-basic notions. *Journal of Computer Science and Cybernetics*, *35*(4), 293–304. https://doi.org/10.15625/1813-9663/35/4/13898
[27] Liu, Z., Sun, Y., Xing, C., Liu, J., He, Y., Zhou, Y., & Zhang, G. (2022). Artificial intelligence powered large-scale renewable integrations in multi-energy systems for carbon neutrality transition: Challenges and future perspectives. *Energy and AI*, 100195. https://doi.org/10.1016/j.egyai.2022.100195
[28] Ramot, D., Milo, R., Friedman, M., & Kandel, A. (2002). Complex fuzzy sets. *IEEE transactions on fuzzy systems*, *10*(2), 171–186. https://doi.org/10.1109/91.995119
[29] Alkouri, A. M. J. S., & Salleh, A. R. (2012). Complex intuitionistic fuzzy sets. *AIP conference proceedings*, *1482*, 464–470. https://doi.org/10.1063/1.4757515
[30] Ullah, K., Mahmood, T., Ali, Z., & Jan, N. (2020). On some distance measures of complex pythagorean fuzzy sets and their applications in pattern recognition. *Complex Intelligent Systems*, *6*, 15–27. https://doi.org/10.1007/s40747-019-0103-6
[31] Liu, P., Ali, Z., Mahmood, T., & Hassan, N. (2020). Group decision-making using complex q-rung orthopair fuzzy bonferroni mean. *International Journal of Computational Intelligence Systems*, *13*(1), 822. https://doi.org/10.2991/ijcis.d.200514.001

[32] Akram, M., Bashir, A., & Garg, H. (2020). Decision-making model under complex picture fuzzy hamacher aggregation operators. *Computational and Applied Mathematics*, *39*, 1–38. https://doi.org/10.1007/s40314-020-01251-2

[33] Akram, M., Bashir, A., & Edalatpanah, S. (2021). A hybrid decision-making analysis under complex q-rung picture fuzzy einstein averaging operators. *Computational and Applied Mathematics*, *40*, 1–35. https://doi.org/10.1007/s40314-021-01651-y

[34] Dagar, A., Mittal, A., Singh, A., Giri, S., & Rathee, S. (2024). Electrical power plant decision-making by utilizing ifs weighted averaging operator. *2024 International Conference on Intelligent and Innovative Technologies in Computing, Electrical and Electronics (IITCEE)*, 1–4. https://doi.org/10.1109/IITCEE59897.2024.10467655

[35] Mao, Q., Fan, J., Lv, J., Gao, Y., Chen, J., & Guo, M. (2024). A decision framework of offshore photovoltaic power station site selection based on pythagorean fuzzy electre-iii method. *Journal of Renewable and Sustainable Energy*, *16*(2). https://doi.org/10.1063/5.0191823

[36] Ünver, M. (2024). Improved cosine similarity measures and extended topsis for q-rung orthopair fuzzy sets: Applications in green technology selection. 10.32388/EOGFR4.3

[37] Mishra, A., Alrasheedi, M., Lakshmi, J., & Rani, P. (2024). Multi-criteria decision analysis model using the q-rung orthopair fuzzy similarity measures and the copras method for electric vehicle charging station site selection. *Granular Computing*, *9*(1), 1–20. https://doi.org/10.1007/s41066-023-00447-1

[38] Senapati, T., & Chen, G. (2022). Picture fuzzy waspas technique and its application in multi-criteria decision-making. *Soft Computing*, *26*, 4413–4421. https://doi.org/10.1007/s00500-022-06835-0

[39] Kahraman, C. (2024). Proportional picture fuzzy sets and their ahp extension: Application to waste disposal site selection. *Expert Systems with Applications*, *238*, 122354. https://doi.org/10.1016/j.eswa.2023.122354

[40] Hussain, A., Ullah, K., Senapati, T., & Moslem, S. (2023). Complex spherical fuzzy aczel-alsina aggregation operators and their application in assessment of electric cars. *Heliyon*, *9*, e18100. https://www.cell.com/heliyon/pdf/S2405-8440(23)05308-2.pdf

[41] Khan, M., Jan, S., Jan, R., Senapati, T., & Moslem, S. (2023). Complex interval-valued intuitionistic fuzzy decision support system with application to covid-19 healthcare facilities. *Complex & Intelligent Systems*, 1–30. https://doi.org/10.1007/s40747-023-01090-8

[42] Kumar, S.-M., & Chen, S. (2024). Multiattribute decision making based on q-rung orthopair fuzzy yager prioritized weighted arithmetic aggregation operator of q-rung orthopair fuzzy numbers. *Information Sciences*, *657*, 119984. https://doi.org/10.1016/j.ins.2023.119984

[43] Liu, P., Shahzadi, G., & Akram, M. (2020). Specific types of q-rung picture fuzzy yager aggregation operators for decision-making. *International Journal of Computational Intelligence Systems*, *13*(1), 1072–1091. https://doi.org/10.2991/ijcis.d.200717.001

[44] Javeed, S., Javed, M., Shafique, I., Shoaib, M., Khan, M., Cui, L., Askar, S., & Alshamrani, A. (2024). Complex q-rung orthopair fuzzy yager aggregation operators and their application to evaluate the best medical manufacturer. *Applied Soft Computing*, *157*, 111532. https://doi.org/10.1016/j.asoc.2024.111532

[45] Wang, W., & Feng, Y. (2024). Group decision making based on generalized intuitionistic fuzzy yager weighted heronian mean aggregation operator. *Int. J. Fuzzy Syst.* https://doi.org/10.1007/s40815-023-01672-1

[46] Yager, R. R. (2001). The power average operator. *IEEE Transactions on Systems, Man, and Cybernetics - Part A: Systems and Humans*, *31*(6), 724–731. https://doi.org/10.1109/3468.983429

[47] Jana, C., Garg, H., & Pal, M. (2023). Multi-attribute decision making for power dombi operators under pythagorean fuzzy information with mabac method. *Journal of Ambient Intelligence and Humanized Computing*, *14*(8), 10761–10778. https://doi.org/10.1007/s12652-022-04348-0
[48] Ma, L., Jabeen, K., Karamti, W., Ullah, K., Khan, Q., Garg, H., & Yin, S. (2024). Aczel-alsina power bonferroni aggregation operators for picture fuzzy information and decision analysis. *Complex & Intelligent Systems*, 1–24. https://doi.org/10.1007/s40747-023-01287-x
[49] Dhankhar, C., & Kumar, K. (2023). Multi-attribute decision making based on the q-rung orthopair fuzzy yager power weighted geometric aggregation operator of q-rung orthopair fuzzy values. *Granular Computing*, *8*(5), 1013–1025. https://doi.org/10.1007/s41066-023-00367-0
[50] Liu, P., Ali, Z., & Mahmood, T. (2024). Schweizer-sklar power aggregation operators based on complex intuitionistic fuzzy information and their application in decision-making. *Complex & Intelligent Systems*, 1–18. https://doi.org/10.1007/s40747-023-01331-w
[51] Yager, R. (2008). Prioritized aggregation operators. *International Journal of Approximate Reasoning*, *48*(1), 263–274. https://doi.org/10.1016/j.ijar.2007.08.009
[52] Kumar, K., & Chen, S. (2024). Multiattribute decision-making based on q-rung orthopair fuzzy yager prioritized weighted arithmetic aggregation operator of q-rung orthopair fuzzy numbers. *Information Sciences*, *657*, 119984. https://doi.org/10.1016/j.ins.2023.119984
[53] Neelam, R., Bhardwaj, & Arora, R. e. a. (2024). Linguistic q-rung orthopair fuzzy yager prioritized weighted geometric aggregation operator of linguistic q-rung orthopair fuzzy numbers and its application to multiattribute group decision-making. *Granul. Comput.*, *9*, 38. https://doi.org/10.1007/s41066-024-00460-y
[54] Garg, H., & Rani, D. (2023). New prioritized aggregation operators with priority degrees among priority orders for complex intuitionistic fuzzy information. *Journal of Ambient Intelligence and Humanized Computing*, *14*(3), 1373–1399. https://doi.org/10.1007/s12652-021-03164-2
[55] Li, L., Zhang, R., Wang, J., Shang, X., & Bai, K. (2018). A novel approach to multi-attribute group decision-making with q-rung picture linguistic information. *Symmetry*, *10*(5), 172. https://doi.org/10.3390/sym10050172
[56] Britannica, T. E. o. E. (2024). Hermann minkowski [Encyclopedia Britannica]. https://www.britannica.com/biography/Hermann-Minkowski
[57] of New, M., & Renewable Energy (MNRE), G. o. I. (n.d.). Renewable energy in india [[accessed May 25, 2024]]. https://mnre.gov.in
[58] Stock, R., & Sovacool, B. (2024). Blinded by sunspots: Revealing the multidimensional and intersectional inequities of solar energy in india. *Global Environmental Change*, *84*, 102796. https://doi.org/10.1016/j.gloenvcha.2023.102796
[59] Husain, A., Hasan, M., Khan, Z., & Asjad, M. (2024). A robust decision-making approach for the selection of an optimal renewable energy source in india. *Energy Conversion and Management*, *301*, 117989. https://doi.org/10.1016/j.enconman.2023.117989
[60] Kumar, M., Tiwari, R., Kumar, K., Rautela, K., & Safi, S. (2024). Quantitative analysis of hydropower potential in the upper beas basin using geographical information system and mike 11 nedbor afrstromnings model (nam). *Ecohydrology*, e2618. https://doi.org/10.1002/eco.2618
[61] Mohan, I., Panda, A., Volli, V., & Kumar, S. (2024). An insight on upgrading of biomass pyrolysis products and utilization: Current status and future prospect of biomass in india. *Biomass Conversion and Biorefinery*, *14*(5), 6185–6203. https://doi.org/10.1007/s13399-022-02833-2
[62] DGiri, P., Paul, S., & Debnath, B. (2024). A fuzzy graph theory and matrix approach (fuzzy gtma) to select the best renewable energy alternative in india. *Applied Energy*, *358*, 122582. https://doi.org/10.1016/j.apenergy.2023.122582

[63] Shift, C. M. (2024). Ev battery recycling in india: Opportunities and challenges [[accessed May 25, 2024]]. https://cleanmobilityshift.com/ecosystem/ev-battery-recycling-in-india-opportunities-and-challenges/
[64] (IRENA), I. R. E. A. (n.d.[a]). Renewable power generation costs in 2019 [[accessed May 25, 2024]]. https://www.irena.org/publications/2020/Jun/Renewable-Power-Costs-in-2019
[65] on Climate Change (IPCC), I. P. (n.d.). Climate change 2014: Mitigation of climate change [[accessed May 25, 2024]]. https://www.ipcc.ch/report/ar5/wg3/
[66] (IRENA), I. R. E. A. (n.d.[b]). Renewable energy market analysis: Southeast asia [[accessed May 25, 2024]]. https://www.irena.org/publications/2018/Jan/Renewable-Energy-Market-Analysis-Southeast-Asia
[67] (IEA), I. E. A. (n.d.). Energy efficiency 2019: Analysis and outlooks to 2040 [[accessed May 25, 2024]]. https://www.iea.org/reports/energy-efficiency-2019
[68] Garg, H., Ali, Z., & Mahmood, T. (2021). Generalized dice similarity measures for complex q-rung orthopair fuzzy sets and its application. *Complex and Intelligent Systems*, *7*, 667–686. https://doi.org/10.1007/s40747-020-00203-x
[69] Du, Y., Du, X., Li, Y., Cui, J.-x., & Hou, F. (2022). Complex q-rung orthopair fuzzy frank aggregation operators and their application to multi-attribute decision making. *Soft Comput.*, *26*(22), 11973–12008. https://doi.org/10.1007/s00500-022-07465-2
[70] Senapati, T. (2022). Approaches to multi-attribute decision making based on picture fuzzy aczel-alsina average aggregation operators. *Computational and Applied Mathematics*, *41*, 40. https://doi.org/10.1007/s40314-021-01742-w
[71] Du, W. (2020). More on dombi operations and dombi aggregation operators for q-rung orthopair fuzzy values. *Journal of Intelligent & Fuzzy Systems*, *39*(3), 3715–3735. https://content.iospress.com/articles/journal-of-intelligent-and-fuzzy-systems/ifs192052
[72] Garg, H., & Chen, S.-M. (2020). Multiattribute group decision making based on neutrality aggregation operators of q-rung orthopair fuzzy sets. *Information Sciences*, *517*, 427–447. https://doi.org/10.1016/j.ins.2019.11.035